THE ANNUAL HEAT BALANCE OF THE SURFACE 100 METERS OF THE

NORTHWEST GULF OF ALASKA SHELF

RECOMMENDED:

Chairman, Advisory Committee

Program Head

APPROVED:

Vice Chancellor for Research and Advanced Study

Date

THE ANNUAL HEAT BALANCE OF THE SURFACE 100 METERS OF THE NORTHWEST GULF OF ALASKA SHELF

A

THESIS

Presented to the Faculty of the University of Alaska

in Partial Fulfillment of the Requirements

for the Degree of

MASTER OF SCIENCE

By

Thomas J. Weingartner, B.S.

Fairbanks, Alaska

December 1980

ABSTRACT

Oceanographic and meteorologic data collected from 1970 to 1978 on the northern Gulf of Alaska shelf are used to compute monthly heat budgets within the surface 100 m for a composite year. During months of net heat gain, radiation is the primary source. Latent and sensible heat transfer dominate during months of net heat loss. Persistent downwelling is the second most important route for heat loss. During winter, alongshore advection is the principal contributor of heat to this region. Cross-shelf advection and diffusion of heat are of minor importance throughout the year and generally counter each other.

The prevalence of onshore Ekman transport explains the cross-shelf variation in the annual amplitude of heat content and the differential propagation rates of surface temperature anomalies to greater depths.

No significant linear relationships were determined between anomalies of surface heat transfer and sea surface temperature. Several hypotheses are presented to explain this result.

ACKNOWLEDGEMENTS

My education and thesis owe much to the guidance and support of numerous people. I thank Dr. Joe Niebauer, my major advisor, for his assistance throughout these years of study. I deeply appreciate his encouraging me in a variety of oceanographic experiences and his understanding during periods of doubt and anxiety. Gratitude is extended to the rest of my committee, Dr. Thomas C. Royer, Dr. William S. Reeburg and Dr. Tsuneo Nishiyama, for their willingness to advise and discuss oceanography and nearly any other topic with me. Knowing these people has been a personal and professional reward.

Thanks are given to Karl Haflinger, Dave Musgrave, Dr. Jack Colonell, Terry Carpenter, Dave Nebert, Phred Short, Jeanne Lapsa and Ray Hadley for providing ways and means. I especially acknowledge Cydney Hansen, Arlene Vaughn and the cheerful IMS data management personnel for their assistance in the extensive data reduction this study required. I thank Steve Worley who dared me to study physical oceanography. Finally, I thank my family whose efforts over the years are ultimately responsible for my education.

This study and student were supported by federal Sea Grant Office contracts, SG-04-7-158-44006, SG04-8-M01-49 and SG04-M01-187 to the University of Alaska.

TABLE OF CONTENTS

LIST OF FIGURES

LIST OF TABLES

CHAPTER 1

INTRODUCTION

A distinct characteristic of high latitude environments is the large amplitude variations in their physical parameters, particularly temperature. In a region as meteorologically and oceanographically dynamic as the Gulf of Alaska, the year-to-year variations as well as the intra-annual fluctuations in the physical variables can be quite large. This investigation was undertaken to provide fundamental information on the processes governing the transfer of heat on the shelf of the Gulf of Alaska. Some of this information is then used to assess the origin of observed sea surface temperature anomalies within the region.

The motivation for this work arises from a consideration of the important consequences that temperature variations may have in the Gulf of Alaska. Thermal anomalies can have severe implications for the biological organisms endemic to the environment, and consequently on the commercial fisheries. In addition, atmospheric cyclonic activity within the Gulf is thought by Namias (1968) to play a key role in short term climatic fluctuations in the Northern Hemisphere. These low pressure systems are dependent to some extent on heat flux from the ocean to atmosphere. Although these biotic and meteorologic effects of thermal changes within the Gulf are not addressed herein, they do supply some of the incentive for this work.

The results reported here have been made possible by the recent increase in oceanographic data acquired under the auspices of the Outer

Continental Shelf Environmental Assessment Program. In addition, meteorological data have been obtained from an offshore station that is free from orographic effects typical of coastal stations surrounding the Gulf. Using these data sets, this analysis identifies the principal physical processes controlling thermal changes on the Gulf of Alaska shelf.

CHAPTER 2

GENERAL OCEANOGRAPHIC AND METEOROLOGIC CONDITIONS OF THE GULF OF ALASKA

Geography

The Gulf of Alaska is a large semicircular basin (radius of 700 km) bordered on the south (in the vicinity of 48°N) by the North Pacific Current. It is surrounded on all other sides by a broad (60 km) band of steep, high (1-3 km) mountains. The shelf width varies from tens to hundreds of kilometers, and is punctuated by numerous submarine ridges and plunging canyons. In general, the depth increases rapidly offshore, to depths of 150-300 m only 10 km from the coast. The shelf break is characterized by an abrupt descent of the bottom to depths of 2000 to 4000 m.

Climatology

The Gulf of Alaska is dominated by two seasonally varying pressure systems. During summer the subtropical North Pacific High migrates northward and, although not centered over the Gulf, encompasses the whole region. From early September to December, the Aleutian Low deepens in intensity and becomes centered over the western Gulf. In January, the low retrogresses westward, as a possible consequence of downstream blocking by high pressure ridges (Elliot and Smith, 1949). The system gradually weakens throughout the summer and nearly disappears in August over the Chukchi Peninsula. The intensity and frequency of cyclones is indicated by the studies of O'Connor (1964) and

Klein and Winston (1958). They analyzed the northern hemispheric distribution of 5-day mean 700 mb circulation centers and found seasonal vorticity maxima for the Northern Hemisphere over Kodiak in the fall, Kamchatka in the winter and the western Aleutians in the spring.

Notwithstanding the seasonal oscillation in these two pressure systems, the Gulf of Alaska is in all seasons a region of predominantly cyclonic activity (Brower *et al.*, 1977; Klein, 1957). The persistence of this cyclonic activity is depicted in the frequent storms, year-round downwelling along the coast (Livingstone and Royer, 1980) and generally overcast conditions (Brower *et al.*, 1977; Sadler *et al.*, 1976).

The year round prevalence of cyclones within the Gulf is related to the semi-permanent atmospheric front over the North Pacific Ocean (Reed, 1960). This frontal structure results from the strong, latitudinal thermal gradient of the ocean in the vicinity of the Kuroshio-Oyashio confluence zone. The outflow of cold, dry continental air masses from east Asia and Siberia over the sea, subsequently modified by surface warming, contributes to cyclonic shear and low pressure genesis. These evolving cyclones traverse the North Pacific from Japan to the Bering Sea and/or the Gulf of Alaska. Once in the Gulf, lows tend to stall and fill as a consequence of the obstructing mountain ranges (Plakhotnik, 1964).

Winston (1955) implicated the Gulf as a region of active cyclogenesis especially during the winter months when continental air flows southeast off mainland Alaska and comes into contact with the relatively

warm Gulf water. Such a situation typically develops when a high pressure ridge occurs over the northern Bering Sea and directs arctic air masses southeastward. Under these conditions Winston (1955) estimated the ocean to atmospheric heat flux to be 1130 cal cm^{-2} day^{-1} for a 60 hour period in February 1950. Assuming no advective or diffusive effects and an isothermal water column this heat loss is equivalent to a decrease of about 0.2°C day^{-1} over a 50 m layer.

Vertical air motions associated with cyclones cause continuous downward flow in the rear of the center to bring cool, dry air into contact with the ocean. Subsequent sensible and latent heat extraction from the ocean sustains the cyclone while cooling the sea. This heat transfer is augmented with increasing wind speeds. Livingstone (1979) obtained a significant positive correlation between mean monthly wind speed and the monthly frequency of low pressure systems within the Gulf. Thus, cyclonic activity will have a key influence on thermal modification within the Gulf of Alaska.

Shelf Circulation

Royer (unpub. manuscript) has provided a review of the physical oceanography for the Gulf of Alaska and a more detailed treatment of the following discussion may be found there. The dynamics of the coastal and shelf circulation along the south coast of Alaska are strongly affected by the excess of precipitation over evaporation, runoff and wind stress. In addition, offshore forcing by the westward flowing Alaskan Current and current steering by bottom topography are critical to the circulation.

The Alaskan Current originates as the northward bifurcation of the North Pacific Current. It acts as a dynamic boundary between the shelf and the interior of the Gulf. This current is an integral component in the meridional advection of heat (Wyrtki and Haberland, 1968; Bathen, 1971). The effect of this current on the shelf circulation is thought to be mediated via eddies and meanders induced by topography and variations in wind stress curl (Thomson, 1972). However, a quantitative assessment of the onshore advection of heat, salt and momentum is still lacking.

Observations of these mesoscale features along the shelf break have been reported in several studies. Royer and Muench (1977) identified numerous eddies (50-100 km diameter) that appear to originate from Alaska Current meanders at the shelf break. Hayes' (1979) current meter deployments across the shelf of the northeast Gulf detected large anticyclonic low frequency fluctuations superimposed on a weak mean alongshore (southeast-northwest) flow. However, these eddies were not observed to propagate onto the shelf. Drifter releases by Royer *et al.* (1979) revealed numerous transient and permanent eddies on the shelf between Yakutat and Prince William Sound.

Hayes and Schumacher (1976) and Hayes (1979) investigated seasonal variations in shelf circulation in the northeast Gulf of Alaska. Hayes and Schumacher found local wind stress, bottom pressure and alongshore flow to be significantly coherent in the winter. At this time relatively cold, low salinity surface water flushes the shelf as a consequence of coastal convergence. This process contributes to weaken the

inshore stratification. Hayes and Schumacher concluded that the shelf response was consistent with a barotropic model dominated by storm events on a 2-10 day scale. In early spring the vertical velocity coherences were lower, implying that offshore baroclinic and nonlocal effects became more important. Hayes (1979) correlated the cross-shelf bottom pressure gradient with alongshore velocity for spring and summer seasons. Again the velocity response was explicable in terms of barotropic quasi-geostrophic dynamics, with spring circulation agreeing better than summer.

The increase in baroclinicity from winter through summer is due to a diminution in downwelling and an increase in freshwater runoff (Royer, 1979). Relaxation of downwelling interspersed with more frequent upwelling events is characteristic of the summer (Bakun, 1975a,b; Livingstone and Royer, 1980). At this time subsurface, offshore water is carried onto the shelf. In early summer this water is slightly warmer and more saline than that found inshore at equivalent depths. This subsurface influx of denser water and increasingly dilute surface water (a consequence of runoff) results in an intensification of the vertical stratification from late spring through early fall.

The importance of freshwater addition to the shelf circulation was further demonstrated by Royer (1979). He obtained a significant positive correlation between dynamic height and combined precipitation and runoff. The influence of freshwater is usually greatest in summer and fall when maximum river discharge (late August) and highest precipitation (late September) dilute the upper 100 m. The correlation

is highest inshore over the 0-100 db interval, but is nonsignificant from 100-200 db. Over this lower interval the dynamic height exhibits a significant inverse correlation with wind stress, suggesting that Ekman pumping and suction dominates the lower layer mass distribution.

The drogue studies of Royer *et al.* (1979) reveal that along the coast, surficial freshwater creates a buoyant plume which spreads offshore and entrains subsurface water. The depth of the entrainment layer is about 35 m within 5-10 km of the coast. Seasonal variations in freshwater influx and coastal convergence are expected to vary the plume width. The net effect of this entrainment is to create an offshore flow in the surface layer and upwelling below.

Past Investigations

Numerous investigations of atmosphere-ocean heat transfer processes have been conducted since the pioneer effort of Jacobs (1951) and continue today within such multidisciplinary programs as GARP (Global Atmospheric Research Program) and NORPAX (North Pacific Experiment). The motivation for these studies has been disparate. Jacobs' (1951) and Manabe and Bryan's (1969) work were prompted by global energy balance considerations. Pond *et al.* (1971) and Deardorff (1968) investigated the mechanics and statistics of heat flux. Kraus and Turner (1967) were primarily interested in the development of the seasonal thermocline.

These studies have provided the foundation for the NORPAX project. The primary goal of this program is to provide information on the

energy transfer between ocean and atmosphere such that long range weather forecasts may be improved for the continental United States. The recent studies of Huang (1979) and Haney *et al.* (1978) is illustrative of work in this direction. Comprehensive reviews of ocean-atmosphere interaction are provided by Roll (1964), Haugen (1973), Kraus (1972) and Favre and Hasselmann (1978).

The author is aware of only two publications on the heat budget of the Gulf of Alaska. Merlo (1974) analyzed the heat balance from December through March on the shelf. His study, however, was limited because of a lack of adequate meteorologic and oceanographic data. Clark's (1967) investigations of the North Pacific included the southern portion of the Gulf of Alaska (south of 55°N) exclusive of the shelf. With the recent increase in data the present study analyzes the annual heat balance and anomalous temperature patterns in the northern Gulf of Alaska. No attempt is made to compare these two studies with each other and with the present one as the methods of analysis, data sets and geographical regions are not identical.

CHAPTER 3

METHODS AND DATA

Study Area

The area analyzed in this study lies wihin the inner shelf region of the north central Gulf of Alaska (Fig. 1). Hydrographic data have been collected frequently but aperiodically along the Seward Line since the mid-1970's. This line consists of eleven stations extending from the mouth of Resurrection Bay (59.9°N, 149.5°W) 200 km southeast across the shelf break. These data represent the most temporally intensive sampling effort in the Gulf to date.

The following transport description through the Seward Line is paraphrased from Royer (unpub. manuscript). Flow through this region is characterized by a southwestward (alongshore) coastal jet between the coast and Station 3 (Fig. 1). Transport magnitudes decrease beyond Station 2 but remain oriented in the same direction as the jet. Beyond Station 6 (about 10 km offshore) flow reversals are common and the region is infiltrated by numerous eddies and meanders of the Alaska Current. Further offshore, beyond Station 9, transport magnitudes increase and direction stabilizes (southwestward) as the mainstream of the Alaska Current is approached.

Model of Heat Conservation

The equation expressing the heat balance over a unit surface area is:

$$\frac{\partial Q}{\partial t} = - \bar{v} \cdot \nabla Q + A_H \nabla^2 Q + A_{zQ} \frac{\partial^2 Q}{\partial z^2} \qquad (1)$$

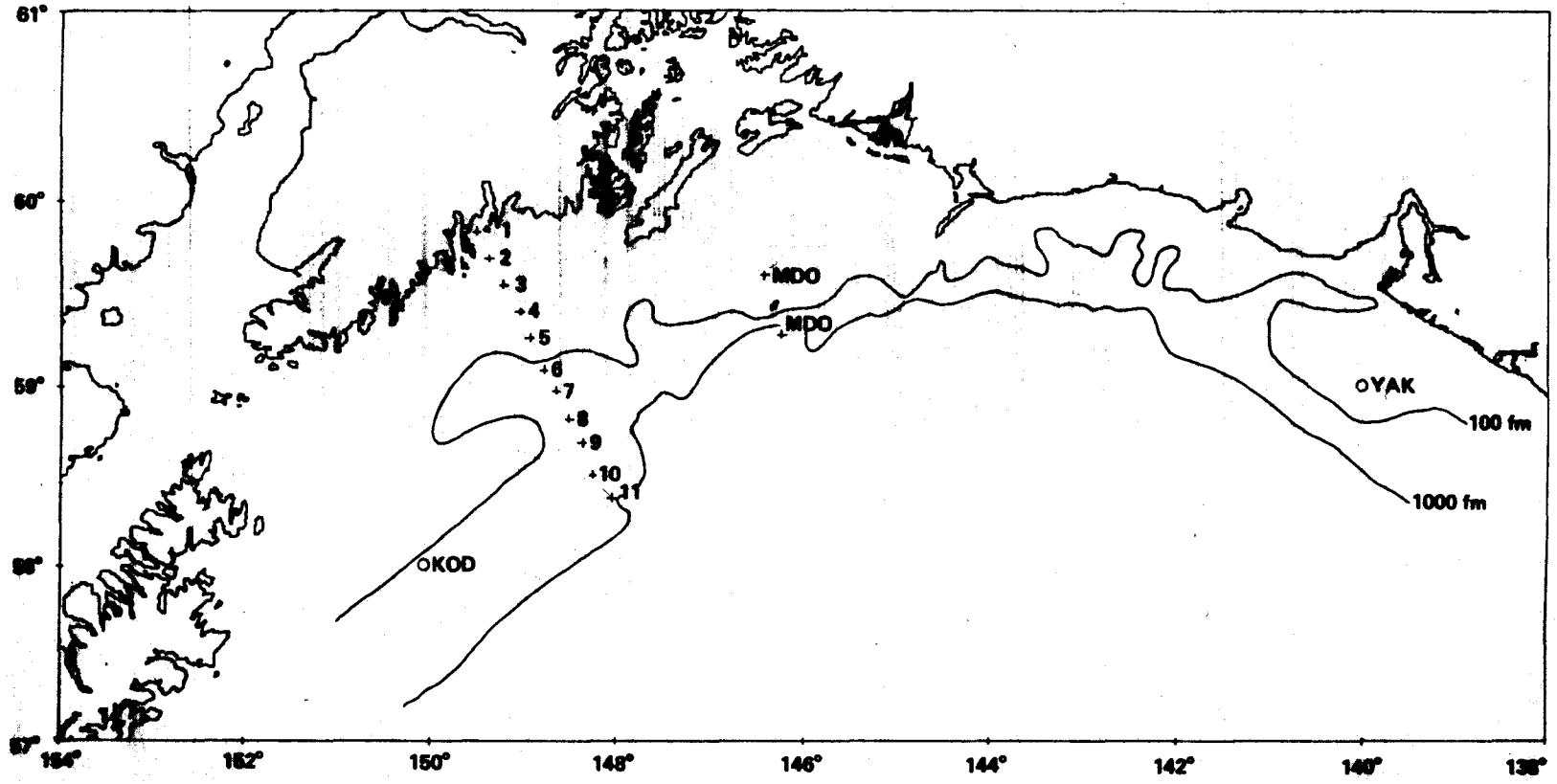

Figure 1. Map of study region. Crosses (+) indicate hydrographic stations used in this study. Station 1 through 11 comprise the Seward Line. Middleton Island lies between the two crosses marked MDO. Kodiak and Yakutat grid centers used for computation of SST by FNWC are represented by the circles (KOD = Kodiak and YAK = Yakutat).

where:

Q = heat storage

$\bar{v}$ = velocity vector

∇Q = gradient of heat content

$\nabla^2 Q$ = horizontal Laplacian content

A_H, A_{zQ} = the horizontal and vertical eddy conductivity coefficients

t = time

A Cartesian coordinate system is used in which x is positive to the east, y is positive to the north and z positive upwards. The corresponding velocity components are u, v, and w.

Integrating eq. (1) over depth D yields

$$D \frac{\partial Q}{\partial t} + \bar{V}_H \cdot \nabla Q - wQ\Big|_D + wQ\Big|_0 = DA_H \nabla^2 Q - A_{zQ} \frac{\partial Q}{\partial z}\Big|_D + A_{zQ} \frac{\partial Q}{\partial Z}\Big|_0 \qquad (2)$$

where $\bar{V}_H$ is the horizontal velocity averaged over the layer. At the boundary $z = 0$, $w = 0$ and $A_{zQ} \frac{\partial Q}{\partial z}$ is the ocean-atmosphere heat exchange, or expanded into its components is:

$$A_{zQ} \frac{\partial Q}{\partial z}\Big|_0 = Q_r + Q_c + Q_\ell \qquad (3)$$

where:

Q_r = surface net radiation flux

Q_c = sensible heat flux

Q_ℓ = latent heat flux

If the depth of integration is chosen such that at depth D, the vertical gradient of heat vanishes, then the last term on the right

side of eq. (2) disappears. Figure 2 is a composite of vertical temperature profiles for different months of the year. The profiles suggest that the vertical temperature gradients decrease sharply below 80 m. Assuming a commonly used value of A_{zQ} to be 10 cm^2 sec^{-1} (Hamilton and Rattray, 1978) at approximately 100 m, the diffusive flux through the bottom of the 100 m layer never exceeds .1 cal cm^{-2} day^{-1}. This loss is, at most, an order of magnitude lower than any of the other fluxes and, therefore, is ignored.

Satellite sea surface thermal analyses provided by Mr. Gary Hufford (NOAA-NESS Anchorage, Alaska) and the work of Royer and Muench (1977) indicate that the alongshore sea surface temperature gradients are smaller than the cross-shelf gradient. Available hydrographic data suggest that the heat gradient is constant along the shelf. Although these data are insufficient to prove that the diffusion gradient is negligible, they do suggest that it is small relative to the other terms in eq. (1) and hence, it is ignored in this study. Using eq. (2), eq. (3) and these results, eq. (1) can be rewritten as:

$$\frac{\partial Q_s}{\partial t} = - v \frac{\partial Q_E}{\partial y} - u \frac{\partial Q_s}{\partial x} + wQ_{100} + A_H \frac{\partial^2 Q_s}{\partial y^2} + Q_r + Q_\ell + Q_c \qquad (4)$$

where Q_s is the heat content calculated over 100 m and Q_{100} is the amount of heat at 100 m. Q_E, in the cross-shelf advection term, is calculated with respect to a time varying depth as will be shown later. Using the available meteorological and oceanographic data estimates are made for all terms in eq. (4) except for the vertical velocity, w, which is solved algebraically.

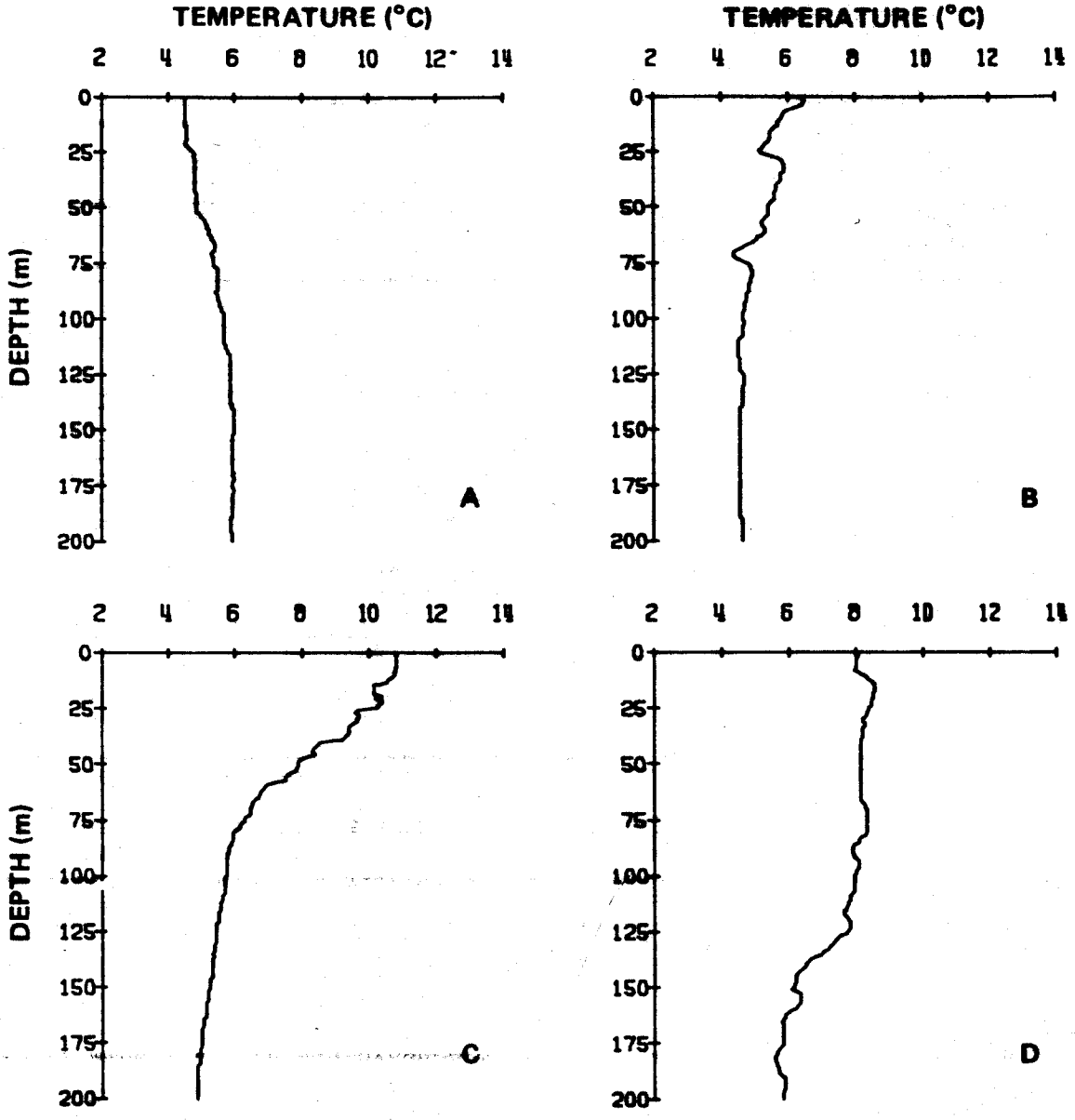

Figure 2. Vertical profiles of temperature at GAK 3 from (A) February 1975, (B) June 1975, (C) September 1975, and (D) November 1976.

Data Sources

This study utilizes 18 hydrographic transects across the Seward Line spanning the period from April 1974 through September 1978. The temporal distribution of these cruises is given in Table I.

Mean monthly sea surface temperature (SST) data for this region was provided by Douglas McLain of the National Marine Fisheries Service, Monterey, California. Monthly mean SSTs are computed from ship of opportunity measurements collected within a 300 by 300 km square centered at 58°N, 150°W (Fig. 1). Missing SSTs were interpolated with a least squares harmonic fit. An additional set of SST data, acquired from the Yakutat area (57°N, 137°W), were used to estimate the alongshore heat gradient.

Wind speed and direction, air temperature and dew point temperature were obtained from the United States Weather Service Automatic Meteorological Observing Station (AMOS) facility on Middleton Island (also referred to as MDO). Middleton Island is a low lying island 8 km long by 1.5 km wide, situated near the shelf break (59°4'N, 146°3'W) about 100 km south of the mainland coast (Fig. 1). The island's low, flat relief minimizes the disturbance of local topographic features on the wind and temperatures (Livingstone and Royer, 1980). The height of the sensors at the AMOS facility are approximately 30 m above sea level. Reynolds' (1978) description of nearshore meteorologic conditions in the northeast gulf for the winter of 1977 suggest that MDO instruments are sufficiently far offshore to be free from coastal influence. His results show that katabatic effects are generally negligible beyond

TABLE I

CRUISES AND DATES OF SEWARD LINE TRANSECTS

Year	Jan	Feb	Mar	Apr	May	Jun	Jul	Aug	Sep	Oct	Nov	Dec
1974			AC186				AC193					
1975		OC805	AC207		RA806	AC212			SB811		SU814	
1976			MW1	MW3			MW5		SU3		FN6	
1977			FN9								DS5	
1978					AC260			AC264	AC266			
			CRUISES AND DATES OF MDO* STATION OBSERVATIONS									
1974							AC193					
1975		OC805	AC207						SB811		SU814	
1976		MW1			RA806				SU3			
1977												
1978					AC260			AC264	AC266			

*Stations located at 59°17.1'N, 146°14.0'W and 59°36.2'N, 146°25.5'W
1978 stations at 59°35.6'N, 146°20.0'W and 59°24.0'N, 146°0'W

Ship Codes:
AC - R/V *Acona*
OC - NOAA Ship *Oceanographer*
RA - NOAA Ship *Rainier*
SB - USNS *Silas Bent*
SU - NOAA Ship *Surveyor*
MW - R/V *Moana Wave*
FN - NOAA Ship *Miller Freeman*
DS - NOAA Ship *Discoverer*

20 km of the coast. In addition, the atmospheric boundary layer appears to be well-mixed in the lower 50 m. As the fall, winter and early spring months are dominated by strong winds, measurements at the height of the MDO sensors are probably representative of conditions close to the sea surface. During summer months, when stable conditions are more frequent, this height can overestimate winds and temperatures close to the sea surface because of vertical velocity shear (Lumley and Panofsky, 1964).

Hourly meteorologic data from 1 June 1972 through 31 December 1978 were used in the computation of sensible and latent heat flux and onshore/offshore Ekman transport. Meteorological data for November 1972 were omitted from the analysis as the number of samples was small and recorded over a short time period. A small cluster of observations could be related to a particular atmospheric weather pattern that may not be representative of the month, hence their use would bias the estimate of the mean monthly heat flux. October and November 1974 had a majority of dew point temperatures greater than air temperatures. Excluding these values from the analysis left a temporally representative set of dew point temperatures and so both months were included. Approximately 50% of the dew point temperatures for September 1972 were less than the overall mean September dew point by more than 4 standard deviations. Exclusion of these values left a small sample, of short duration, hence September 1972 latent heat values were not used.

Mean monthly cloud cover was computed from the frequency histograms for MDO provided by Brower *et al.* (1978) in their atlas. Cloud

cover data for individual months of a given year were not available. The monthly means used in this study represent long term averages. Monthly standard deviations of cloud cover, computed from the data of Sadler *et al.* (1976), are between 15 and 20% of the monthly mean. Although this variance is small compared to the other meteorological parameters, Sadler *et al.* (1976) show that anomalies as great as 20% may occasionally persist for two to three months. Such anomalies may be important during the summer months.

Evaluation of Heat Flux Terms

Heat Storage, Advection and Diffusion

The amount of heat stored in a 100 m layer of water of unit area is calculated according to:

$$Q_s = \rho C_p \int_{100}^{0} T dz \qquad (5)$$

where ρ is the density of seawater, C_p is the specific heat and T is temperature. The quantity ρC_p is assumed to be constant throughout the year and is equal to 0.982 cal cm^{-3} C^{-1}. A mean monthly Q_s for each station was computed from all measurements within a particular month. The monthly means form a composite year and the expected value for a particular month can be estimated from:

$$Q_s(t) = \bar{Q}_s + A \cos(\omega t) + B \sin(\omega t) \qquad (6)$$

Here, $\bar{Q}_s$ is the annual mean, ω is the frequency ($2\Pi/12$) and $t = n-1$ where n is the month number. The coefficients, A and B, are found by

a least squares fit of the data to eq. (6). The statistical significance of the approximation is determined by analysis of variance. Differentiation of eq. (6) with respect to time yields $\frac{\partial Q_s}{\partial t}$. $\frac{\partial Q_E}{\partial y}$ and $\frac{\partial^2 Q_s}{\partial t^2}$ are calculated by finite difference.

Because the sample size is small for any particular month and the monthly mean is based on samples scattered over different times of the month, the variance associated with a particular monthly mean is high enough that statistically significant differences between adjacent stations are not resolved. This implies that little reliability could be associated with the cross-shelf gradient terms. To determine the smallest grid size appropriate to estimate advective and diffusive terms the mean monthly Q_s for station pairs was compared using a Student's t-test. The 1974-1978 data set was augmented with 5 additional transects obtained in 1979. (These transects were not used in any other analyses because concurrent SST and MDO data were lacking.) The t-test revealed that in general no two station pairs nor every other station pair were significantly different from each other. In 67% of the cases Stations 1 and 4 were significantly different and 33% of the cases indicated that Stations 3 and 6 were significantly different ($P > .1$ where P is the significance level). In all cases, Stations 1 and 5 or 1 and 6 were significantly different ($P > .1$). On the basis of these results, the advective term was computed by differencing Stations 1 and 6 and the diffusion term computed between 1 and 6 and centered at the average of 3 and 4. Thus, the minimum distance in which differences in heat content can be reasonably ascertained with

this data set is about 65 km. Data from Stations 3 and 4 were averaged and the heat balance computed for this station (hereafter written as 3.5). Okubo and Ozmidov (1970) determined an empirical relationship between the coefficient of eddy diffusivity and the size of the grid scale. From their results a value of A_H was chosen equal to 3.0×10^6 cm^2 sec^{-1}.

The cross-shelf velocity, v (defined below), is assumed to be wholly dependent upon the cross-shelf Ekman transport. Although this assumption is consistent with Hayes' (1979) inability to relate cross-shelf flow to the alongshore pressure gradient, it ignores eddy momentum flux and the onshore/offshore velocity component of the shelf circulation. Generally the alongshore circulation coincides with isobaths, which are parallel to the coast. There are two topographic features in the vicinity of the Seward Line that would accelerate the onshore/offshore velocity components. Upstream, a small ridge (40 km long), running perpendicular to the coastline, rises to about 100 m. Downstream, the bottom shoals to a depth of about 150 m. Conservation of potential vorticity requires the presence of an onshore flow on the lee side of the ridge and an offshore component on the near side of the shoals. Hence, the cross-shelf velocity, as defined here, is only a crude approximation of the flow perpendicular to the coast.

Livingstone and Royer (1980) calculated the steady state wind drift transport using MDO data for the period 1972 to 1976. The same computational scheme outlined in their paper was applied to 1977 and

1978 MDO wind data. Once the mass transport has been computed the mean velocity in the Ekman layer can be determined from:

$$v = \frac{M_y}{\rho D_E} \tag{7}$$

where D_E is the Ekman depth and M_y is the meridional wind induced mass transport.

The mean monthly Ekman depth is determined by

$$D_E = \pi \left(\frac{A_z}{\rho \Omega \sin \phi}\right)^{1/2} \tag{8}$$

Here A_z is the vertical eddy viscosity and is determined from the empirical relationship given by Neumann and Pierson (1966, p. 196):

$$A_z = .1825 \times 10^{-4} \, u^{5/2} \tag{9}$$

where u is the wind speed. Using eqs. (8) and (9) the mean monthly Ekman depths are about 70 m for October through February, 50 m for March, April, May, and September and 35 m for June through August. These depths represent an upper bound for the Ekman layer as eq. (9) assumes a constant A_z with depth. This approximation is assumed valid for a neutrally stable water column. Frequently, A_z is parameterized as a function of the Richardson number (Hamilton and Rattray, 1978) and is depth dependent.

An accurate evaluation of the alongshore advection term is difficult because the complicated shelf circulation patterns are poorly understood and synoptic hydrographic surveys of the region are sparse. For this reason, the alongshore gradient was computed in two ways. The

first method used mean monthly SSTs at Kodiak and Yakutat. Because SSTs are assumed to represent the average mixed layer temperature for the month, the heat content is computed by integrating the SST over the mixed layer depth. In this study the mixed layer is assumed equivalent to the Ekman depth. Implicit in this assumption is that below the mixed layer the temperatures of the Kodiak and Yakutat squares are equivalent. Hydrographic data collected along the Seward and Yakutat Lines indicate that this approximation is not unwarranted (Royer, 1975). Between 60 and 100 m the temperatures across the shelf for both of these lines are nearly the same. Only in summer are the temperatures below the prescribed mixed layer depth (35 m) higher (by about 1°C) along the Yakutat Line than the Seward transect. The second method utilized data from two stations near Middleton Island and GAK 3.5. The Middleton Island stations were occupied sporadically during the period of this study.

These stations are between 100 and 250 m deep. Heat content was computed by integrating over 100 m according to eq. (5) and averaging the values. Table I lists the times of occupation for these stations. These stations may not be representative of the upstream heat content as they lie near a zone of shoals surrounding Middleton Island. One further complication is that coastal water east of Kayak Island is directed offshore by this island and probably passes through the area wherein these stations lie (Royer, unpub. manuscript). The alongshore velocity within the upper 100 m was obtained from the transport estimates across Stations 2 through 5 of the Seward Line as computed by Royer (1980).

Radiation

Reed (1977) reviewed the numerous empirical methods published for the estimation of incident radiation. He compared clear sky insolation data collected at nonurban coastal stations with the various formulae. The observations agreed best with the relation determined by Seckel and Beaudry (1973). In the same paper, Reed (1977) developed an empirical relation from 40 months of radiation data for cloud corrected insolation. His results were applied in this study to compute cloud corrected insolation. Incident radiation is further reduced by the reflectivity of the sea surface. Albedo values were chosen for 60°N from Kondratyev (1972, Table 2-19). Net longwave radiation was determined after Reed (1976). The sum of albedo and cloud corrected insolation and the longwave emission gives an estimate of the net incident radiation penetrating the sea surface. As the lower limit of the control volume (i.e., 100 m) is well beyond the depth of light penetration, all the radiation is absorbed within this layer.

Sensible and Latent Heat Flux

The bulk aerodynamic formulae are used for computing sensible and latent heat exchange. Although these formulae are operationally simple to use there is considerable uncertainty as to their accuracy. Theoretically, the time averaged vertical flux of any property within the medium is given by:

$$F = - \rho \overline{w' m'} \qquad (10)$$

where F is the flux, $\overline{w'm'}$ is the time averaged correlation of the vertical velocity (w') and the constituent (m') and ρ is the density. Turbulence introduces complications in the transfer process which are empirically contained in a transfer coefficient, i.e., eq. (10) is rewritten as

$$F = - \rho K \frac{\partial \bar{m}}{\partial z} \tag{11}$$

where K is the eddy transfer coefficient. Integration of eq. (11) over a height, z, yields the gradient as a finite difference. K is denoted as the product of a dimensionless drag coefficient (C_D) and the wind speed, u (Businger, 1972). This representation is the bulk aerodynamic method:

$$F = - \rho C_D u(\Delta \bar{m}) \tag{12}$$

For the specific cases of heat and moisture flux over the sea, eq. (12) is

$$Q_c = - \rho C_{pa} C_c (\bar{T}_s - \bar{T}_a) \bar{U}_a \tag{13}$$

and

$$Q_\ell = - \rho L C_\ell (\bar{q}_s - \bar{q}_a) \bar{U}_a \tag{14}$$

where:

T_s = sea surface temperature

T_a = air temperature at height a

q_s = specific humidity at the sea surface (assumed saturated at T_s)

q_a = specific humidity at the atmosphere at height a

C_{pa} = specific heat of dry air

L = heat of vaporization

C_c = transfer coefficient for sensible heat

C_ℓ = transfer coefficient for moisture

In general the exchange coefficients are not equal and both will vary depending upon atmospheric stability, sea state and height of the measurements above the sea surface. Of particular importance is the influence of stability. Because the production of turbulent kinetic energy is a function of the shear stress and the vertical heat flux, vertical heat transfer is enhanced under a regime of high wind shear or positive buoyancy flux. These conditions are typical of the fall through early spring seasons in the gulf when the ocean warms the overlying air and strong winds prevail. When the ocean is cooler than the atmosphere, stable conditions ensue and the wind shear and buoyancy terms are of opposite sign. High wind speeds overcome the stratification effects by enhancing atmospheric mixing.

Although much theoretical and experimental effort has been expended to unravel the transfer properties under a wide range of atmospheric situations, the quest for unambiguous results has been hampered by instrumental and logistical obstacles. Friehe and Gibson (1978) reviewed much of the heat flux data gathered from atmospheric profiles. They solved for the exchange coefficients by computing the slope of the line established by relating the eddy fluxes to the finite difference form. Their values are:

$$\overline{w'q'} = C_\ell u_a(\Delta q);\ C_\ell = 1.32 \times 10^{-3};$$

$$\overline{w'T'} = A + C_c u_a(\Delta T)$$

for $u(\Delta T) < 25$ mK sec^{-1} $A = .002$ mK sec^{-1} and $C_c = .97 \times 10^{-3}$; for $(\Delta T) > 25$ mK sec^{-1} $A = 0$ and $C_c = 1.46 \times 10^{-3}$.

These values are fairly constant over a wide range of conditions. This outcome is counter to the semi-empirical hypotheses of Deardorff (1968) and Kondo (1975). Both of these authors predict a greater variation in the exchange coefficients than that determined by Friehe and Gibson. This discrepancy may be traced to data artifacts (see Friehe and Gibson, 1978), unknown to earlier researchers, introduced by the instruments. However, Friehe and Gibson state that the best available data are not adequate to rigorously test the early hypotheses. In addition to the above papers and references cited herein, the interested reader is directed to the volume edited by Favre and Hasselmann (1978) for a more thorough discussion of this subject.

Aside from the difficulty involved in determining the exchange coefficients, the nonlinear nature of eqs. (13) and (14) tend to enhance error propagation. These errors may become especially serious when average values are chosen for a long time period (i.e., a month). If mean monthly wind speed is perfectly correlated with air temperature and specific humidity the error will be minimized. Decreased significance of the correlation will severely impair the accuracy of the estimated flux. Hourly data from MDO was used to compute the heat flux and then averaged for the month to determine the mean monthly heat flux. Alternately, mean monthly values of temperature, wind speed and humidity were used to estimate the mean monthly heat flux. Unfortunately, the SST data set consists only of monthly means so that

the variability in monthly heat exchange is due solely to the meteorological variables. However, SST is much less variable over the course of a month than any of the atmospheric parameters.

The aerodynamic formulae have not been evaluated for extreme storms for practical reasons, hence their applicability to such conditions is subject to question. The latent heat formula neglects the evaporation of sea spray; an effect which is poorly understood but potentially important (Weng and Street, 1978).

Error Analysis

The maximum random error associated with ocean temperature measurements is 0.02°C (Wooster and Taft, 1958). Hence the maximum error associated with the calculation of Q_s over 100 m is about 196 cal cm^{-2} or 1.96 cal cm^{-2} m^{-1} of integration. Assuming no error in station spacing (i.e., 18.53 km distance is constant) the possible errors in the first and second spatial derivatives are about 10% and 40% respectively.

The MDO wind speed and direction sensors are accurate to within 50 cm sec^{-1} and 10° (Anonymous, 1976). As a consequence, the mean Ekman layer velocity estimate has an associated random error of 10%. This velocity estimate ignores the probability that the depth of the Ekman layer is overestimated and the uncertainty of using a constant drag coefficient for the calculation of momentum transfer. The combined errors in the velocity and gradient variables give a possible error in the cross-shelf advective term of at least 20%.

Reed (1977) estimates the error in mean monthly net incident radiation as 10%. Clark (1967) judges the error in long-wave radiation to be approximately 5% on the average. Most of this error is due to cloud cover assessments.

The uncertainties in the conductive and latent heat flux calculations are extremely large. The AMOS facility has an accuracy of ± 0.55°C for air temperatures. The accuracy of the dew point temperatures are considerably poorer. For dew points greater than -1.1°C the true dew point temperature is within ± 0.83°C. For dew points less than -1.1°C the uncertainty grows to ± 1.4°C (Anonymous, 1976). In conjunction with the wind speed accuracy, errors as great as 50% can be generated in the latent and sensible heat flux estimates. Sensible heat flux is consistently less reliable than latent, partially due to the variable transfer coefficient of the former. The error in latent heat flux varies seasonally from a fall-winter low of 15% to a summer maximum of about 40%. This seasonal dependency is due to the nonlinear relationship between temperature and humidity. For example, at low temperatures, a 1°C change produces a smaller change in saturation vapor pressure than a comparable temperature difference at higher temperatures. Table II summarizes the errors associated with each estimate in the heat budget equation. Note that the least reliable estimates for sensible and latent heat transfer are found in the summer.

TABLE II

SUMMARY OF PERCENT RANDOM ERROR ASSOCIATED WITH EACH TERM OF EQUATION 4

Variable	Random Error
Q_r	10%
$v\ \partial Q_E/\partial y$	20%
$\partial^2 Q_s/\partial y^2$	40%
Q_ℓ	15% (Oct-Jan)
Q_ℓ	25% (Feb-Apr)
Q_ℓ	40% (May-Sep)
Q_c	25% (Oct-Feb)
Q_c	50% (Mar-Sep)

CHAPTER 4

RESULTS

The results of the heat balance computations are summarized in Figures 3 through 10 and Tables III through VII. Table III contains the magnitudes of the monthly values for the individual terms of eq. (4). Table IV lists the percent contribution of each term to the monthly balance. Table V expresses the results of Table III for the entire composite year. In spite of the relatively large uncertainty in the estimates of the various terms, some general conclusions can be drawn. The following discussion is based on the results of eq. (4) using SST data to compute the alongshore advection of heat. The reasoning for this choice is deferred until the following section.

Figure 3 illustrates the seasonal signal in heat storage, Q_s, and $\frac{\partial Q_s}{\partial t}$. The annual amplitude in Q_s is about 40 kcal cm^{-2} with a maximum of 80 kcal cm^{-2} in September and October and a minimum of 40 kcal cm^{-2} during March and April.

The derivative, $\frac{\partial Q_s}{\partial t}$, lags Q_s by three months and is very nearly in phase with the net radiation term, Q_r (Fig. 4). Q_r is the dominant heat source for the ocean from March through September. It accounts for more than 80% of the heat influx from April through August. From November to January there is a net loss of heat via long wave emission as solar altitude is diminished. Net radiation supplies from 10 to 20% of the heat influx during the months of February and October.

Both sensible and latent heat flux show strong annual periodicities (Fig. 5). Together they account for the majority of the heat

TABLE III

SUMMARY OF MONTHLY HEAT BUDGET TERMS AND VERTICAL VELOCITIES FOR COMPOSITE YEAR

Month	$\frac{\partial Q_s}{\partial t}$	=	Q_s	+	Q_ℓ	+	Q_c	$\frac{v\partial Q_E}{\partial y}$	+	$\frac{u\partial Q}{\partial x}$	+	$\frac{A_H \partial^2 Q_s}{\partial y^2}$	+	wQ_{100}
Jan	-360		-29		-151		-117	29		28 [-37]		-46		-74 [-116]
Feb	-269		15		-97		-42	58		68 [42]		-50		-221 [-97]
Mar	-106		88		-89		-35	27		25		-42		-80
Apr	82		205		-81		-16	27		24 [99]		-28		-49 [-125]
May	254		310		-46		10	14		19		-8		-45
June	354		367		-33		15	1		23 [130]		10		[-29] [-141]
July	360		351		-17		16	-1		34 [180]		22		-45 [-151]
Aug	269		262		-45		2	-3		32 [294]		24		-3 [-233]
Sep	106		137		-88		-9	-13		76		18		-15
Oct	-82		34		-140		-50	-15		107 [67]		2		-20 [-51]
Nov	-254		-23		-135		-80	-14		94		-18		-78
Dec	354		-38		-170		-91	4		60		-26		-93

Heat flux units are $cal\text{-}cm^{-2}\ day^{-1}$.
Number in brackets is the value derived from using MDO hydrographic stations to compute alongshore gradient.

TABLE IV

PERCENT CONTRIBUTIONS OF HEAT EXCHANGE TERMS TO MONTHLY HEAT BALANCE
(BASED ON SST DATA)

Month	Heat flux cal cm^{-2} day^{-1}	Q_r	Q_ℓ	Q_c	$\frac{v\partial Q_E}{\partial y}$	$\frac{u\partial Q}{\partial x}$	$A_h\frac{\partial^2 Q_s}{\partial y^2}$	wQ_{100}
January								
Influx	57				50	50		
Efflux	-417	7	36	8			11	18
$\frac{\partial Q_s}{\partial t}$	-360							
February								
Influx	141	11			41	48		
Efflux	-410		24	10			12	54
$\frac{\partial Q_s}{\partial t}$	-269							
March								
Influx	140	63			19	18		
Efflux	-246		36	14			17	33
$\frac{\partial Q_s}{\partial t}$	-106							
April								
Influx	256	80			11	9		
Efflux	-174		47	9			16	28
$\frac{\partial Q_s}{\partial t}$	82							
May								
Influx	353	88		3	4	5		
Efflux	-99		46				8	46
$\frac{\partial Q_s}{\partial t}$	254							
June								
Influx	416	89		4	<1	6	1	
Efflux	-62		53					47
$\frac{\partial Q_s}{\partial t}$	354							
July								
Influx	423	85		4		8	3	
Efflux	-63		27		2			71
$\frac{\partial Q_s}{\partial t}$	360							

TABLE IV

CONTINUED

Month	Heat flux cal cm^{-2} day^{-1}	Q_r	Q_ℓ	Q_c	$v\frac{\partial Q_E}{\partial y}$	$u\frac{\partial Q}{\partial x}$	$A_h\frac{\partial^2 Q_s}{\partial y^2}$	wQ_{100}
August								
Influx	320	82		1		10	7	
Efflux	-51		88		6			6
$\frac{\partial Q_s}{\partial t}$	269							
September								
Influx	231	62				34	4	
Efflux	-125		70	8	10			12
$\frac{\partial Q_s}{\partial t}$	106							
October								
Influx	143	24				75	1	
Efflux	-225		62	22	7			9
$\frac{\partial Q_s}{\partial t}$	-82							
November								
Influx	94					100		
Efflux	-348	7	39	23	4		5	22
$\frac{\partial Q_s}{\partial t}$	-254							
December								
Influx	64				6	94		
Efflux	-418	9	41	22			6	22
$\frac{\partial Q_s}{\partial t}$	-354							

ANNUAL

Influx Variable	cal cm^{-2} yr^{-1} ($\times 10^5$)	Period during which 75% of term's flux occurs
Radiation	6.13	May - August
Cross-shelf advection	0.42	Jan - Feb
Alongshore advection	2.15	Sept - Mar

Efflux Variable	cal cm^{-2} yr^{-1} ($\times 10^5$)	Period during which 75% of term's flux occurs
Evaporation	3.99	Sept - Mar
Conduction	1.45	Oct - Feb
Cross-shelf diffusion	0.52	Jan - Feb
Vertical advection	2.74	Nov - Apr

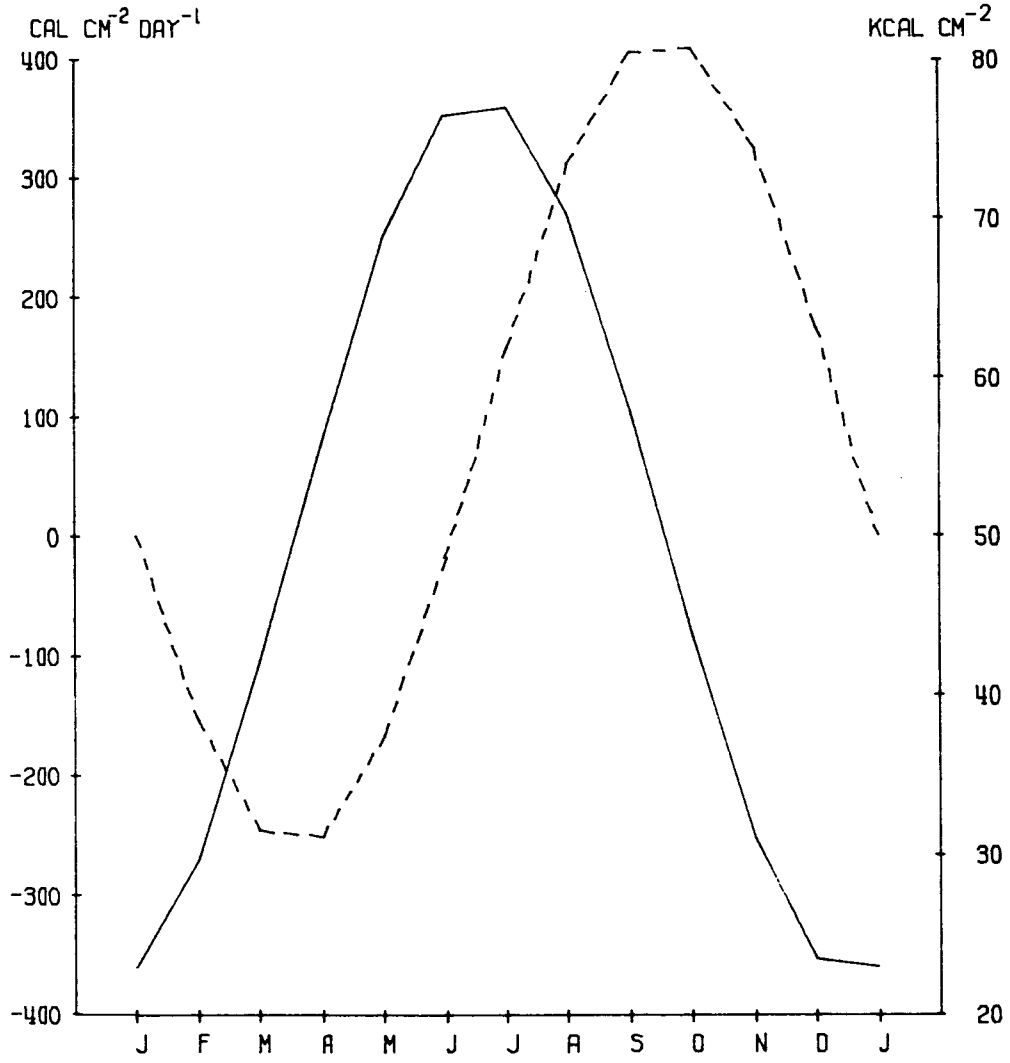

Figure 3. Annual cycle of heat storage, Qs (kcal cm^{-2}) in the 0-100 meter layer (dashed line). Solid line is the monthly mean daily rate of change of Qs, $\frac{\partial Qs}{\partial t}$ (cal cm^{-2} day^{-1}).

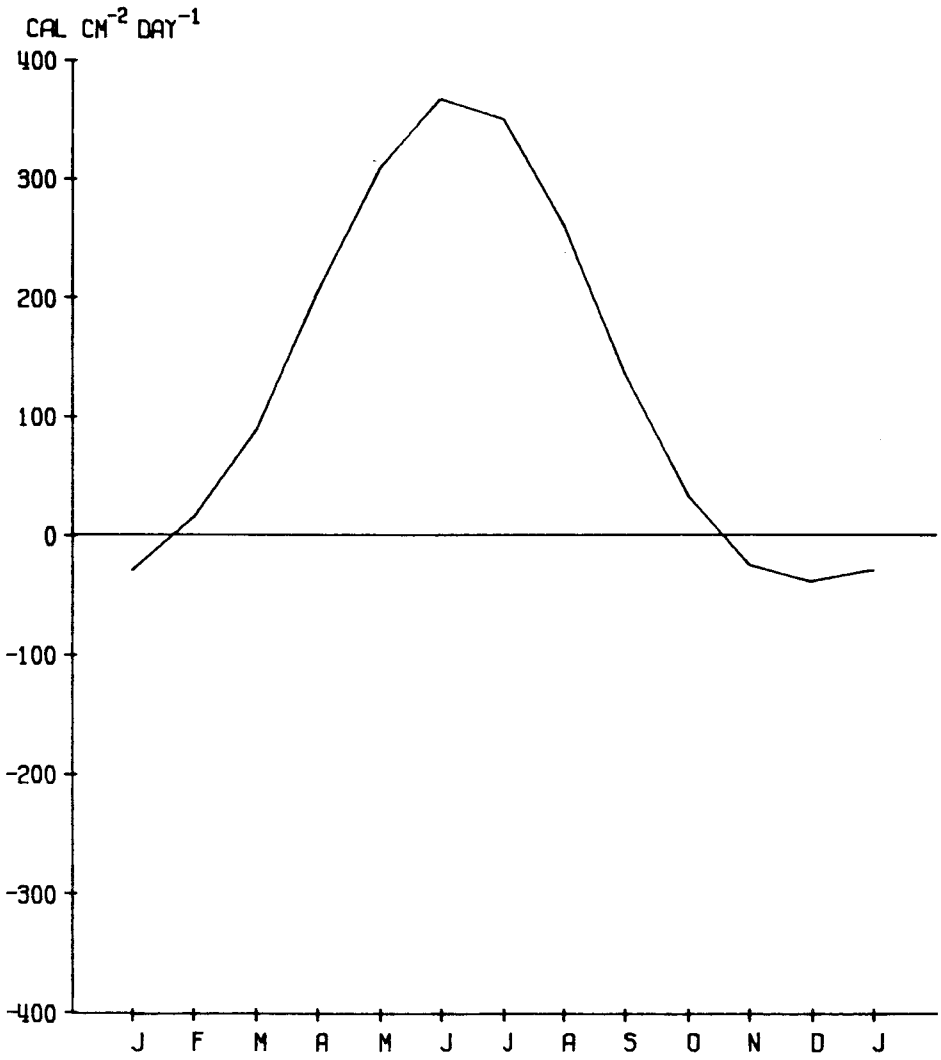

Figure 4. Monthly mean daily net radiation flux, Q_r.

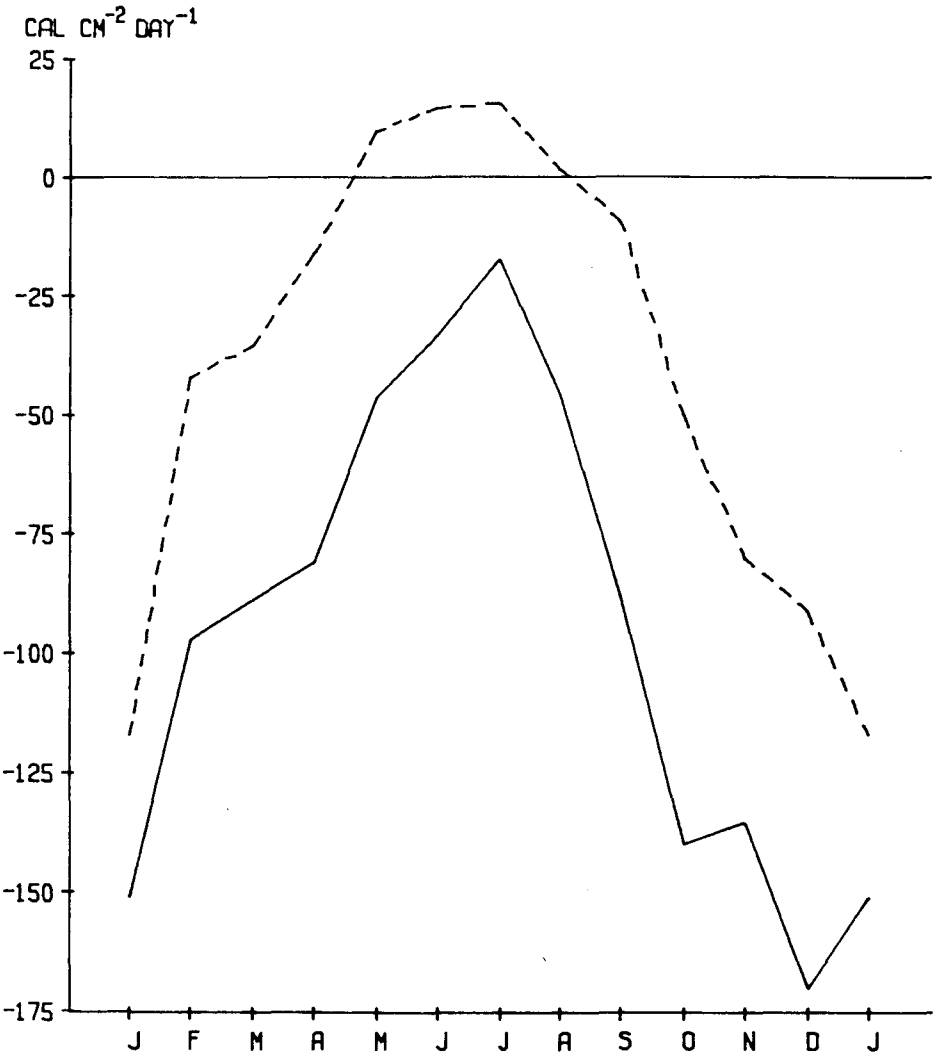

Figure 5. Monthly mean daily latent (solid line) and sensible (dashed line) heat exchange.

loss from September through April (exclusive of February). Evaporation is 1.5 to 3 times more important than the conductive heat loss from October through March, 5 times as great in April and 10 times as great in September. During the summer months, the magnitude of latent heat loss is small although it accounts for 27 to 88% of the heat loss from May to August. The ocean receives a small gain of heat via conduction during these months, however, this influx never amounts to more than 4% of the total.

Table VI summarizes the differences in the mean monthly latent and sensible heat fluxes computed from hourly and monthly meteorological data. The differences for Q_{ℓ} are within the error of the measurements for all months. In general, the magnitudes of latent heat loss based on mean monthly meteorological variables are higher than those obtained using hourly data. While differences in sensible heat exchange, using monthly averages, are within the accuracy of the data, the high standard deviation suggests that the use of mean monthly data will frequently result in errors in excess of the accuracy of the data. Use of mean monthly wind speed and temperature data does not consistently under or overestimate the sensible heat exchange.

The cross-shelf advection and diffusion of heat are shown in Figure 6. Both exhibit a definite annual signal although their respective maxima and minima occur at different times. Advection is nearly 180 degrees out of phase with diffusion and, in general, the magnitude of the diffusive heat flux is greater. Only in June and November are these terms of the same sign. The inverse relationship between the two

TABLE VI

MEAN PERCENT DIFFERENCE BETWEEN MEAN MONTHLY LATENT AND SENSIBLE HEAT FLUX CALCULATED FROM HOURLY METEOROLOGICAL DATA AND MEAN MONTHLY METEOROLOGICAL DATA:

$$\% \text{ difference} = \frac{\bar{Q}_{\text{monthly}} - \bar{Q}_{\text{hourly}}}{Q_{\text{hourly}}} \times 100$$

	Mean Q_ℓ	std. dev.	Mean Q_c	std. dev.
January	7.2	3.4	18	20
February	15	7.0	-15	21
March	13	7.0	-6	26
April	7	11.0	1	115
May	3	14.0	4	30
June	-8	36	-6	35
July	3	10	21	35
August	-3	7	33	46
September	5	8	10	93
October	6	12	-25	28
November	11	11	-2	31
December	4	3	-4	23

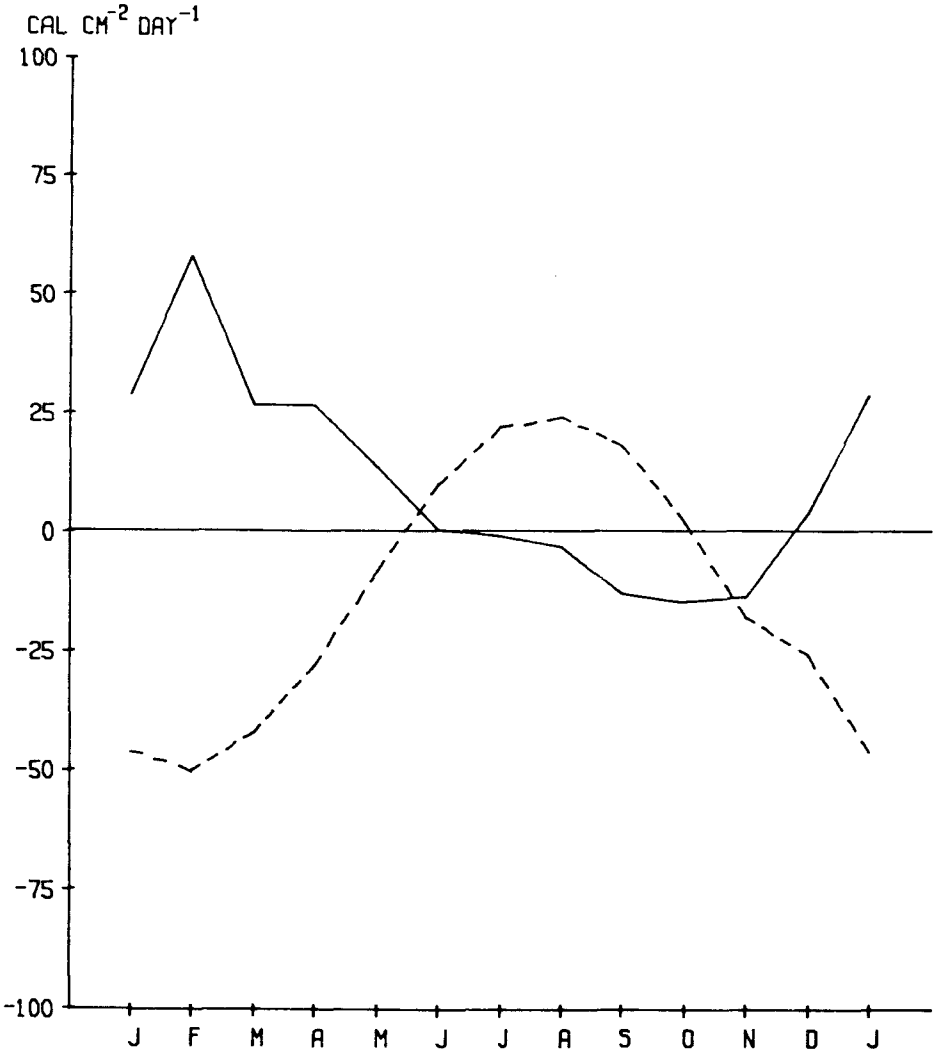

Figure 6. Monthly mean daily cross-shelf advective (solid line) and diffusive (dashed line) heat flux.

is a consequence of coastal convergence and will be discussed more fully in the following chapter.

Onshore advection and diffusion of heat play a minor role in the heat balance of the shelf throughout the year. Cross-shelf advection accounts for approximately 50% of the heat influx in January and decreases rapidly to near negligible levels by June. From July to November offshore water is advected towards the coast and cools the area. This influx of cooler water represents 1 to 10% of the total heat loss. The small diffusive influx of heat occurs from June through October and never exceeds 7% of the total heat gain. From November through May heat diffuses out of the area, but again the magnitudes are small.

Figure 7 illustrates the monthly alongshore heat gradient computed from mean monthly SST data (solid line) and MDO hydrographic stations (open circles). The alongshore velocity (averaged over 100 m), as calculated from transport data, is shown by the dashed line. Figure 8 shows the monthly alongshore advective heat flux based on the values in Figure 7. Calculations based on the SST data indicate that this flux is positive throughout the year and is the most important heat source for Station 3.5 from October through February. During the spring and summer months this flux accounts for less than 10% of the total heat gain.

In comparison the MDO derived terms show striking differences. Apart from February, March and November the hydrographic data yield estimates 2 to 5 times the SST data for the alongshore advection term.

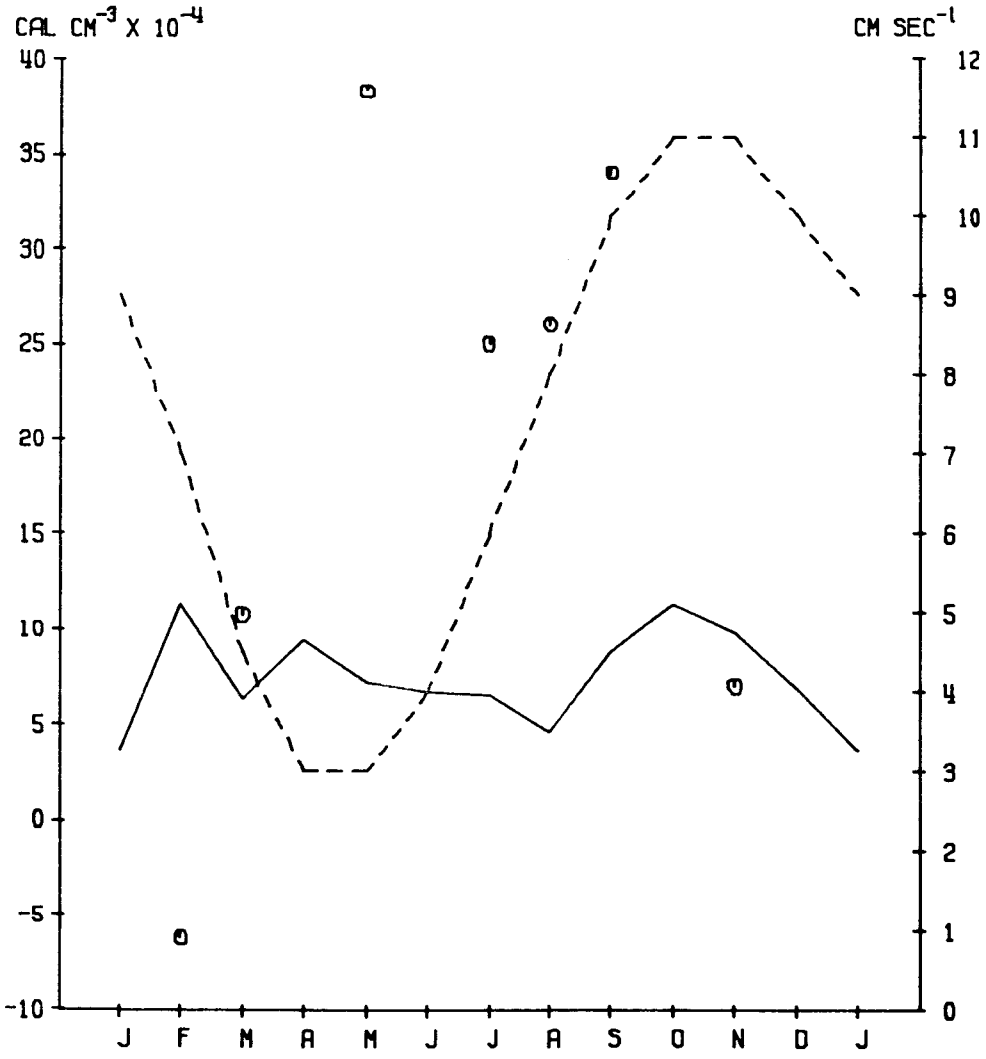

Figure 7. Mean monthly alongshore heat gradient, $\frac{\partial Qs}{\partial x}$. Solid line represents gradient computed from SST data, circles depict gradient computed from MDO hydrographic stations. Dashed line represents mean monthly alongshore velocity, u, in the 0-100 m layer.

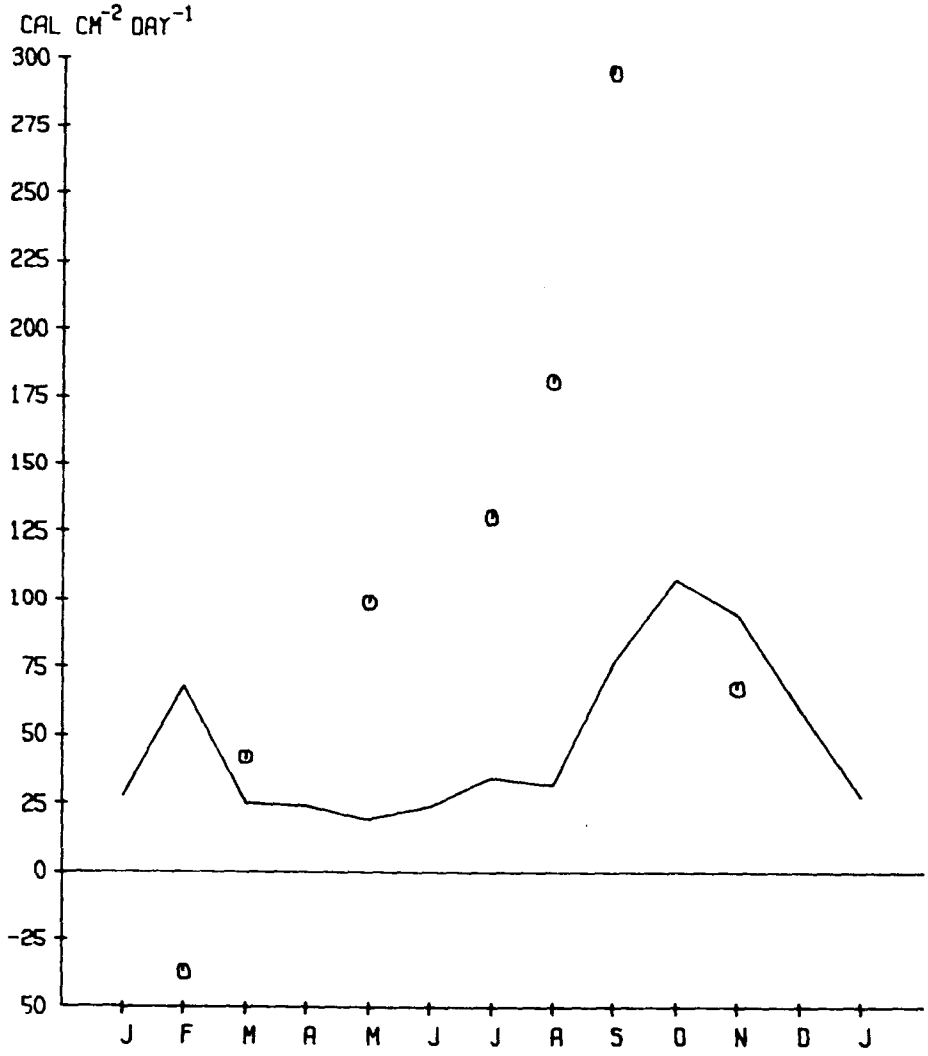

Figure 8. Mean monthly alongshore advection of heat, $u \frac{\partial Qs}{\partial x}$. Solid line and circles same as in Figure 7.

In February this gradient is negative. While some of the discrepancies between the two estimates for this gradient can be attributed to the choice of the mixed layer depth, the MDO stations may not be a good representation of the heat content for this region of the shelf. Further evidence in support of this contention is presented in the next section.

The derived vertical heat advection term is shown in Figure 9. The solid line is the result calculated from eq. (4) using mean monthly SST data and the circles are the results using MDO station data. In either case the loss of heat through the bottom of the 100 m layer represents a substantial fraction of the total heat loss for all months of the year except August through October. From November through July this efflux accounts for 22 to 72% of the total heat loss in the water column. Vertical heat loss calculated from the MDO station estimates are substantially higher than those estimated from SST data for the summer months.

The mean monthly vertical velocities for Station 3.5 are listed in Table VII. These velocities range from a minimum of -6×10^{-4} cm sec^{-1} in February to a maximum of -1×10^{-5} cm sec^{-1} in August. The annual variation of w (determined from SST data and the MDO stations), and the mean monthly upwelling indices (from Bakun, 1975a,b) are plotted together in Figure 10. The apparent annual variation in w, as determined from SST data, reflects the seasonality of coastal convergence. Vertical velocities derived from the MDO stations are more constant with time.

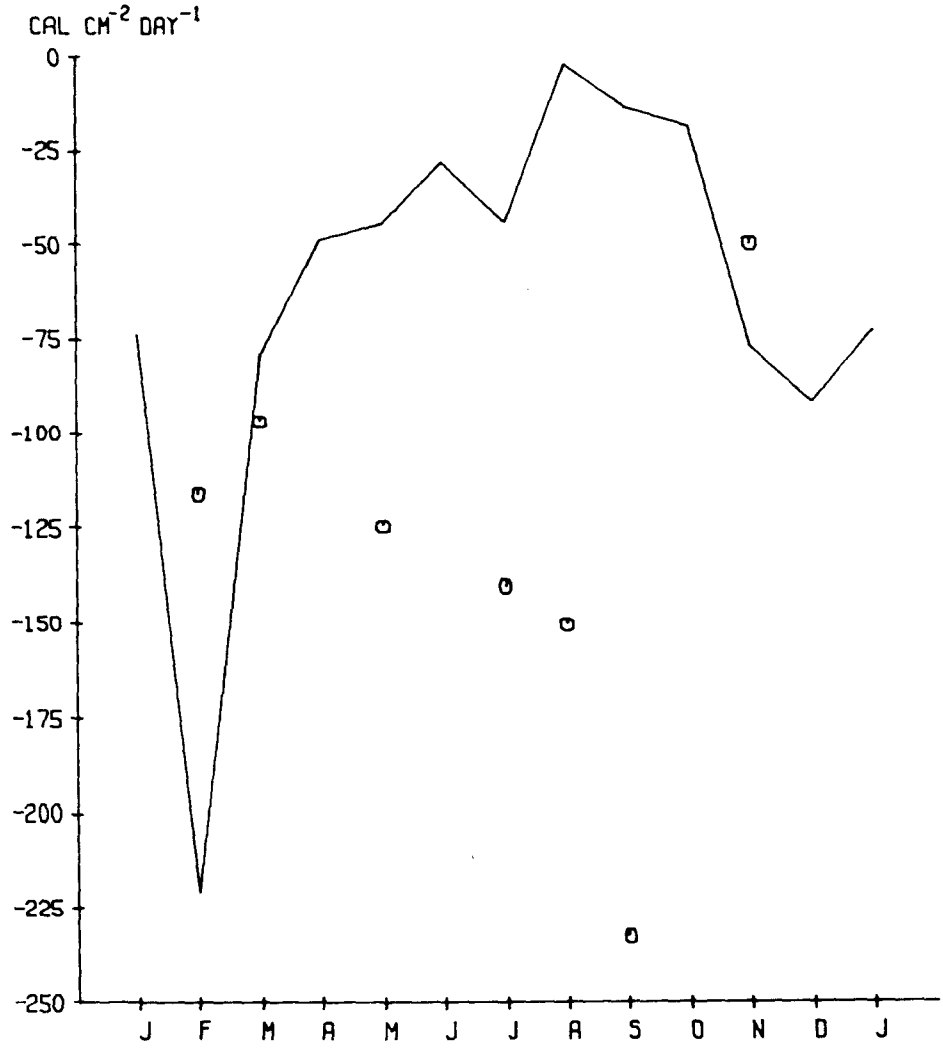

Figure 9. Mean monthly vertical advection of heat. Solid line and circles are the same as in Figure 7.

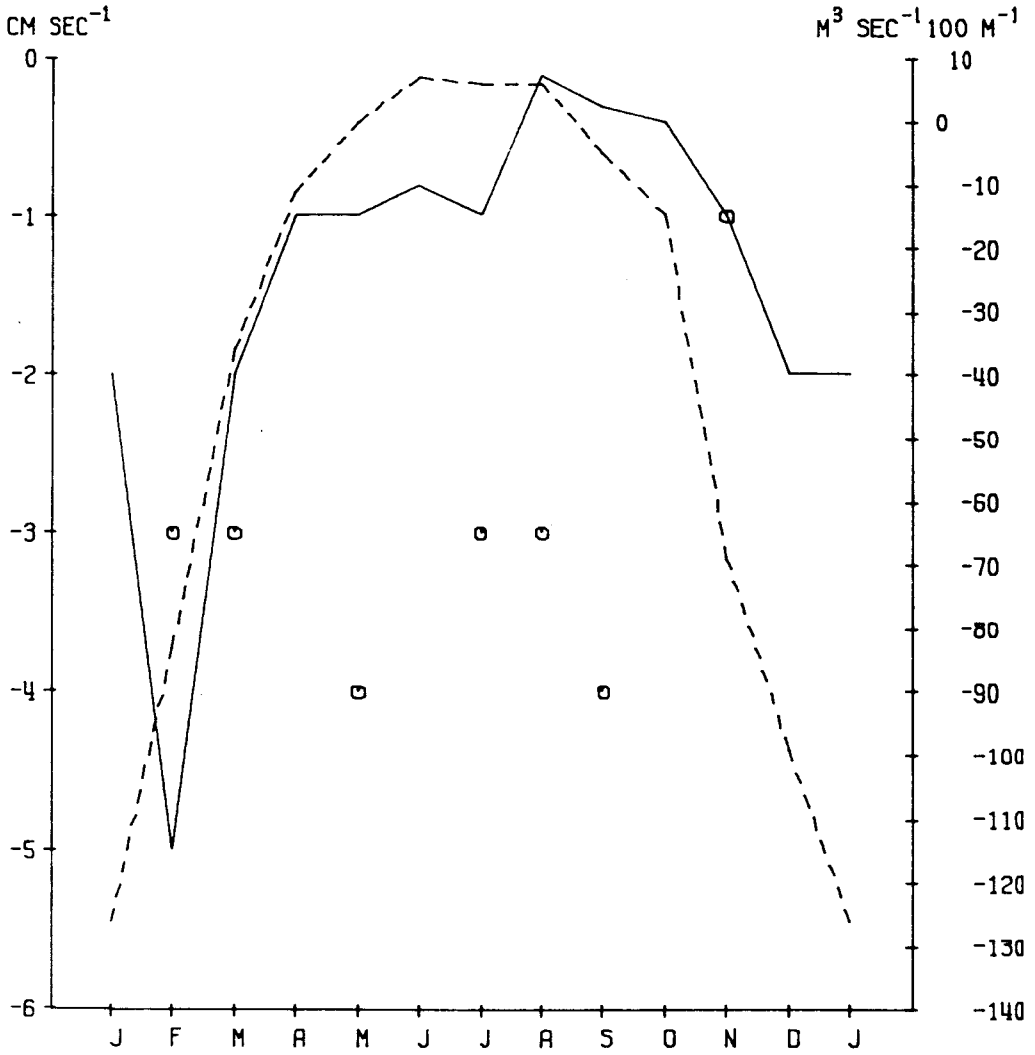

Figure 10. Mean monthly vertical velocity at 100 m derived from equation 4. Solid line and circles as in Figure 7. Dashed line represents the mean monthly upwelling indices computed from 1946-1973 (Bakun, 1975a and pers. comm.).

TABLE VII

MEAN MONTHLY VERTICAL VELOCITIES FOR COMPOSITE YEAR
($cm\ sec^{-1} \times 10^{-4}$)

Jan	Feb	Mar	Apr	May	Jun	Jul	Aug	Sep	Oct	Nov	Dec
-2	-5	-2	-1	-1	-.8	-.1	-.1	-.3	-.4	-1	-2
	(-3)	(-3)		(-4)		(-3)	(-3)	(-4)		-1	

Terms in parentheses are velocities determined from MDO hydrographic station data.

The derived velocities appear to be in phase (Fig. 10) with the annual cycle of onshore Ekman transport. However, because of the random errors associated with the individual terms in eq. (4) these derived values are at best within 1.2 to 10 times the reported value. Given these limitations in accuracy, it is not possible to resolve monthly differences in the vertical velocities with the present data set.

These velocities are in reasonably good agreement with values reported in the literature. Huang's (1978) model results yield typical values of about -10^{-4} cm sec^{-1} for downwelling regions of the open ocean. Arthur (1965) suggested values of 6×10^{-4} cm sec^{-1} for upwelling velocities 50 to 100 km off the coast. Station 3.5 is approximately 65 km from shore and is outside the zone of coastal convergence (the deformation radius has an annual maximum of 28 km in late summer). Within the scale length of the radius of deformation coastal upwelling velocities are on the order of 10^{-2} to 10^{-3} cm sec^{-1} (Bryden, 1978; Wooster and Reid, 1963).

CHAPTER 5

DISCUSSION

Relations Between Ocean Thermal Anomalies and Air-Sea Heat Flux Anomalies

The preceding results show that surface heat exchange dominates the annual heat balance on the northwest Gulf of Alaska Shelf. During months of net heat gain, net radiation (Q_r) is the major source of heat. The atmosphere is the major heat sink during months of net heat loss when latent (Q_ℓ) and sensible heat (Q_c) exchange dominate the heat budget.

Because of the importance of the air-sea heat transfer terms in the heat budget of the shelf, anomalous sea surface temperatures may originate from or generate anomalous atmosphere-ocean heat fluxes. Past investigations have suggested numerous mechanisms by which anomalous surface heat flux generates ocean thermal anomalies and vice versa. Namias (1963, 1970) suggests that, among other factors, interannual differences in seasonal cloud cover distributions may cause ocean thermal anomalies via abnormal radiative flux. White and Barnett (1972) related changes in atmospheric relative vorticity to the Laplacian of the ocean-atmosphere heat flux within the Kuroshio-Oyashio confluence. Winston (1955) demonstrated the significance of the Gulf of Alaska as a heat source for the intensification of cyclonic development. White and Clark (1975) described the importance of anomalous sensible heat flux to the onset of baroclinic instability in the overlying atmosphere of the mid-latitude North Pacific. Davis (1976)

examined monthly SST and sea level pressure (SLP) anomalies and concluded: 1) SST anomalies can be predicted with significant skill from the previous month's SLP anomaly; 2) SLP anomalies for a given month can be specified from the simultaneous SST and 3) SLP anomalies cannot be predicted from the previous month's SST anomaly. In summary, his observations imply that on a monthly time scale the atmosphere controls the oceanic thermal regime. Huang's (1979) model results suggest that anomalous surface heat exchange may be primarily responsible for the genesis of SST anomalies at high latitudes.

In light of these past researches and the importance of predicting atmospheric and oceanic features, several hypotheses are tested concerning SST anomalies (SST') within the Gulf of Alaska. These hypotheses are tested by computing the correlation between SST' and the anomaly of the dominant surface heat flux term. In computing these correlations consideration must be given to the time response of the ocean to atmospheric events. Since oceanic conditions are the result of the integrated effects of the atmosphere, SST anomalies are unlikely to immediately reflect anomalous surface heat exchange. Huang (1979) determined that 3 months is the approximate e-folding response time for a 70 m deep mixed layer subjected to abnormal surface heat flux. In accordance with this time scale, anomalous surface heat fluxes were averaged over the three months prior to the observed SST anomaly and the correlation computed. In comparison to the ocean, the atmosphere responds on the order of a few days to heat exchange with the ocean. Significant correlations between SST', cloud cover anomalies (CC') and

latent plus sensible heat anomalies ($Q'_{\ell c}$) could reflect the result of the ocean modifying the atmosphere or, in agreement with Davis's (1976) conclusion, the atmosphere controlling the ocean. Correlations were also computed between anomalous surface heat flux within a month and anomalous ΔSST' (ΔSST' is the anomalous SST change between two adjacent months) computed from the SST difference between the current month and the following month. ΔSST' should more realistically reflect the effect of an anomalous monthly heat flux than SST' because of the aforementioned response time of the ocean to the atmosphere.

Cloud cover anomalies for May through August were obtained from the atlas of Sadler *et al.* (1976) for the years 1962-1972 and May through July of 1973. Sensible and latent heat flux anomalies were derived from the MDO data discussed earlier.

Table VIII summarizes the correlation results. No significant correlations ($P > .05$) were computed between summer CC' with simultaneous SST', ΔSST', or fall SST'. Similarly three month averages of $Q_{\ell c}$, correlated with monthly SST' did not yield any significant correlations for the year, nor for the combined fall, winter and spring months. $Q_{\ell c}'$ and ΔSST' showed no significant correlations. Finally, there is, in general, no significant correlation between zero lagged $Q_{\ell c}'$ and SST' (except December) and SST' lagged one month behind $Q_{\ell c}'$ (except January and February). Caution is advised in accepting the significant correlations as valid as they arise from only two extremely anomalous years in all cases. Recomputing the correlation, exclusive of these two years, yields a nonsignificant correlation. Because of

TABLE VIII

CORRELATIONS BETWEEN ANOMALOUS SST AND ATMOSPHERIC HEAT FLUX VARIABLES

(r = the correlation coefficient; df = degrees of freedom)

Correlation		Jan	Feb	Mar	Apr	May	June	July	Aug	Sep	Oct	Nov	Dec
$Q'_{\ell c}$ vs ΔSST'	r	.12	.63	-.67	-.25					-.25	.41	.22	.69
	df	2	3	3	2					3	3	3	2
$Q'_{\ell c}$ vs SST' (lag = 0)	r	-.17	.54	-.62	-.67					-.13	-.20	-.63	-.92*
	df	3	3	3	3					3	5	4	4
$Q'_{\ell c}$ vs SST' (lag = -1)**	r	.66	.95*	.87*	-.46	-.77				.29	.12	.56	-.67
	df	2	3	3	2	3				3	3	4	3
$Q'_{\ell c}$ vs SST' (lag = +1)***	r	.60	.15	-.83	-.75	.57				-.47	.48	-.89*	.60
	df	3	3	3	3	4				4	4	4	3
CC' vs ΔSST'	r						-.15	-.08	-.17	-.21			
	df						7	7	6	6			
CC' vs SST'	r					.21	.29	.29	.22				
	df					7	7	7	6				
3 month $\overline{CC'}$ vs SST'	r								-.23	.20			
	df								6	6			

3 month $Q'_{\ell c}$ vs SST' for all months r = -.08, df = 61.
3 month $Q'_{\ell c}$ vs SST' for Sept. through May r = .19, df = 30.

* P > .05.
** $Q'_{\ell c}$ precedes SST' by 1 month.
*** SST' precedes $Q'_{\ell c}$ by 1 month.

the small sample size for many of these tests, the conclusion that there is no apparent relationship between SST' and anomalous surface heat flux must be regarded as tentative. However, the validity of this conclusion gathers further support when considering the proximity of the Alaskan Current as well as other dynamic forces operating within the gulf.

As previously mentioned, the Gulf of Alaska gyre is an important component in the poleward advection of heat. Secular fluctuations in the transport of the subarctic gyre have been described by White (1977), although the magnitude of the changes are unknown. SST anomalies within the gulf may be a reflection of these transport variations. An equally possible cause is that thermal anomalies generated elsewhere in the North Pacific may ultimately arrive in the gulf as a consequence of permanent ocean wide current systems. Local effects within the gulf may also be critically involved in the formation of SST anomalies. The topography of the northwestern gulf is conducive to the formation of meanders and eddies. Variations in wind stress curl on monthly or seasonal bases are thought to be instrumental in generating instabilities within the boundary current of the Gulf of Alaska (Thomson, 1972). Smith (1978) demonstrated the importance of Gulf Stream eddies on the flux of heat onto the Scotian Shelf. He estimated that on an annual basis eddies may contribute an amount of heat equivalent to 30% of the yearly solar input. Douglas McLain (unpub. data, NOAA-NMFS, Monterey, California) computed autocorrelations of SST anomalies for the eastern, northeastern and northwestern Gulf of Alaska. For the

eastern and northeastern regions anomalies persist for nearly eighteen months, whereas in the northwestern gulf the correlation drops off sharply within about six months. This lack of persistence may be attributable to enhanced horizontal mixing by eddies, meanders and the stronger horizontal velocity shear as the Alaska Current assumes the characteristics of a western boundary current in the northwestern gulf.

SST anomalies may also be closely linked with freshwater addition into the gulf as suggested by Royer and Muench (1977). Within the gulf salinity predominantly effects density and stratification. Shelf water is progressively diluted due to the accumulation of runoff and precipitation as it flows around the gulf. Since the depth of the mixed layer is a function of wind stress and stratification, thermal anomalies may be a consequence of enhanced (or inhibited) mixing. Ocean-atmosphere models will have to incorporate this salinity effect in order to properly simulate heat transfer in this region.

Effects of Coastal Convergence on the Shelf Heat Distribution

The importance of coastal convergence on the cross-shelf distribution of heat (integrated over 100 m) is illustrated in Figures 11 through 15. In Figures 11 through 13 mean monthly heat quantities (Q_S) are plotted for the stations along the Seward Line. These months are chosen as representative of the seasonal thermal characteristics on the shelf. The lower curve of Figure 11 shows the spatial distribution for March which is typical of the period from February through May. For this period, Q_S and Q_E (not shown) increase logarithmically in the offshore

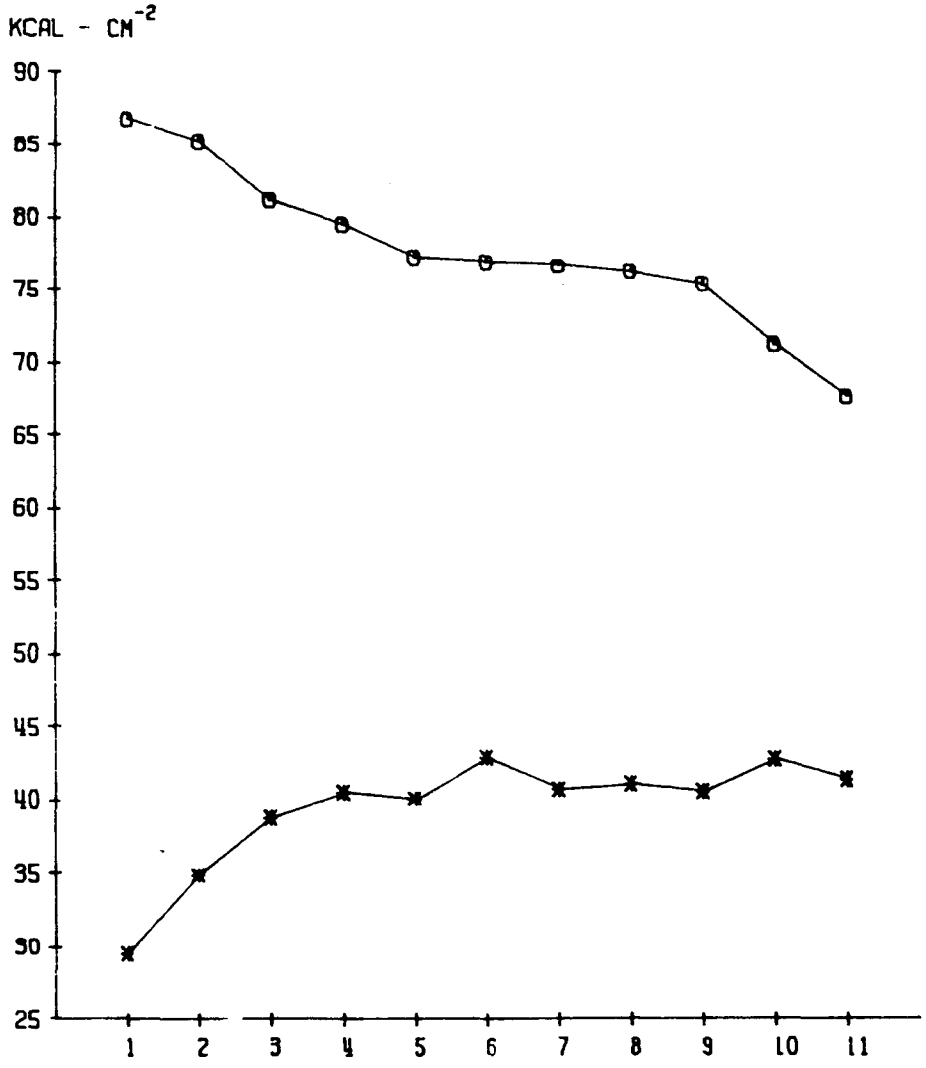

Figure 11. Cross-shelf distribution of Qs (0-100 m) along Seward Line for March (asterisks) and September (circles). Distance offshore increases from station 1 to 11.

direction and can be described reasonably well by a curve of the form:

$$Q = a + b(\ln y)$$

where y increases in the offshore direction. Values of $r^2 > .80$ were computed for these months except February when $r^2 = .48$. This equation is consistent with the signs of the cross-shelf advective and diffusive terms (i.e. $\partial Q_E/\partial y \alpha y^{-1}$ and $\partial^2 Q_s/\partial y^2 \alpha -y^{-2}$). From August through October (exemplified by September in the upper curve of Fig. 11), Q_s and Q_E (not shown) can be expressed by:

$$Q = a - b(\ln y)$$

with an $r^2 > .80$ for these months. Note again that the first and second derivatives of this expression with respect to y yield gradients of opposite sign (i.e. $\partial Q_E/\partial y \alpha -y^{-1}$ and $\partial^2 Q_s/\partial y^2 \alpha y^{-2}$). The remaining months of the year can be categorized as transitional between late winter and late summer. For example, the cross-shelf distribution of heat in the upper 50 m of the shelf in June (Fig. 12) is evolving toward the pattern that exist in September. The 50-100 m distribution of heat retains some of the characteristics of the winter pattern, most notably the cold water close to the coast. From November through January (depicted by December in Fig. 13), the warmest water is found close to the coast in the 50-100 m layer. The upper 50 m are nearly isothermal across the shelf except close to the coast where the water is coldest.

These seasonal patterns are explicable in terms of coastal convergence and surface heat exchange. As downwelling is persistent (although

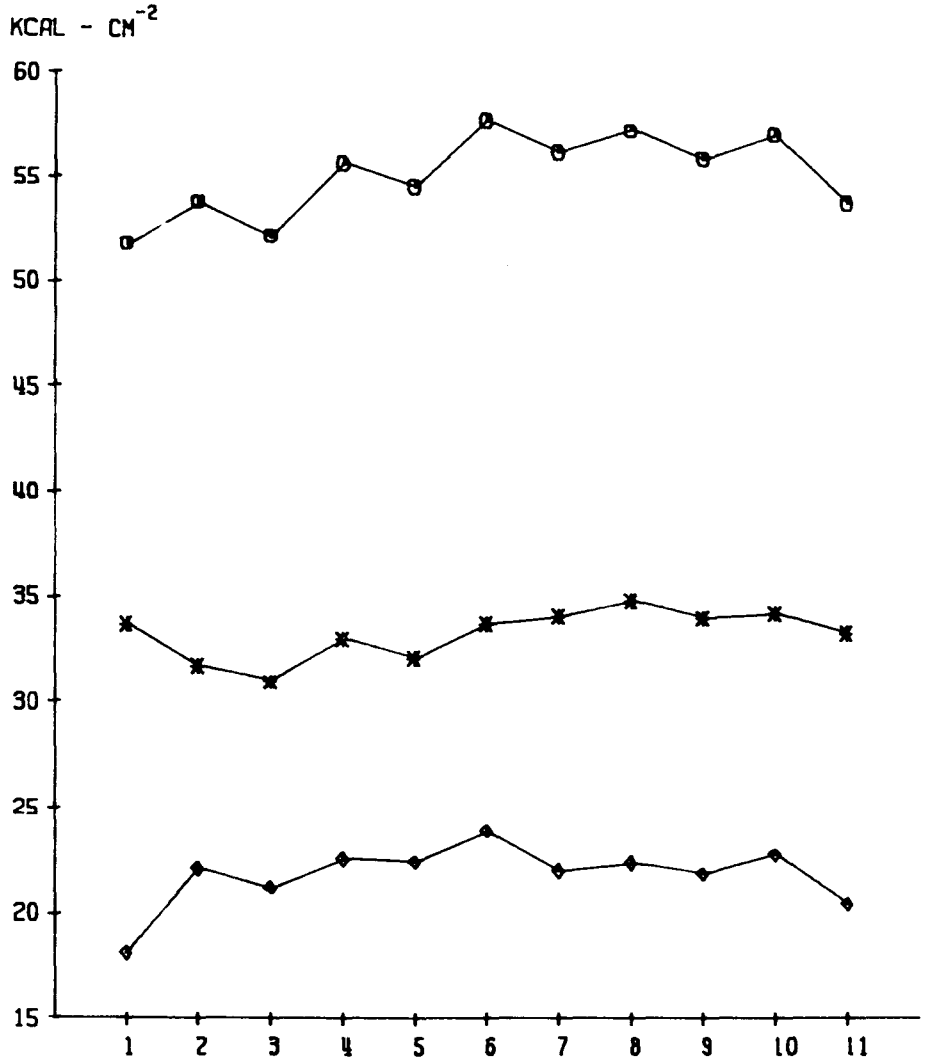

Figure 12. Cross-shelf distribution of Qs along Seward Line for June. 0-100 m indicated by circles, 0-50 m by asterisks and 50-100 m by diamonds.

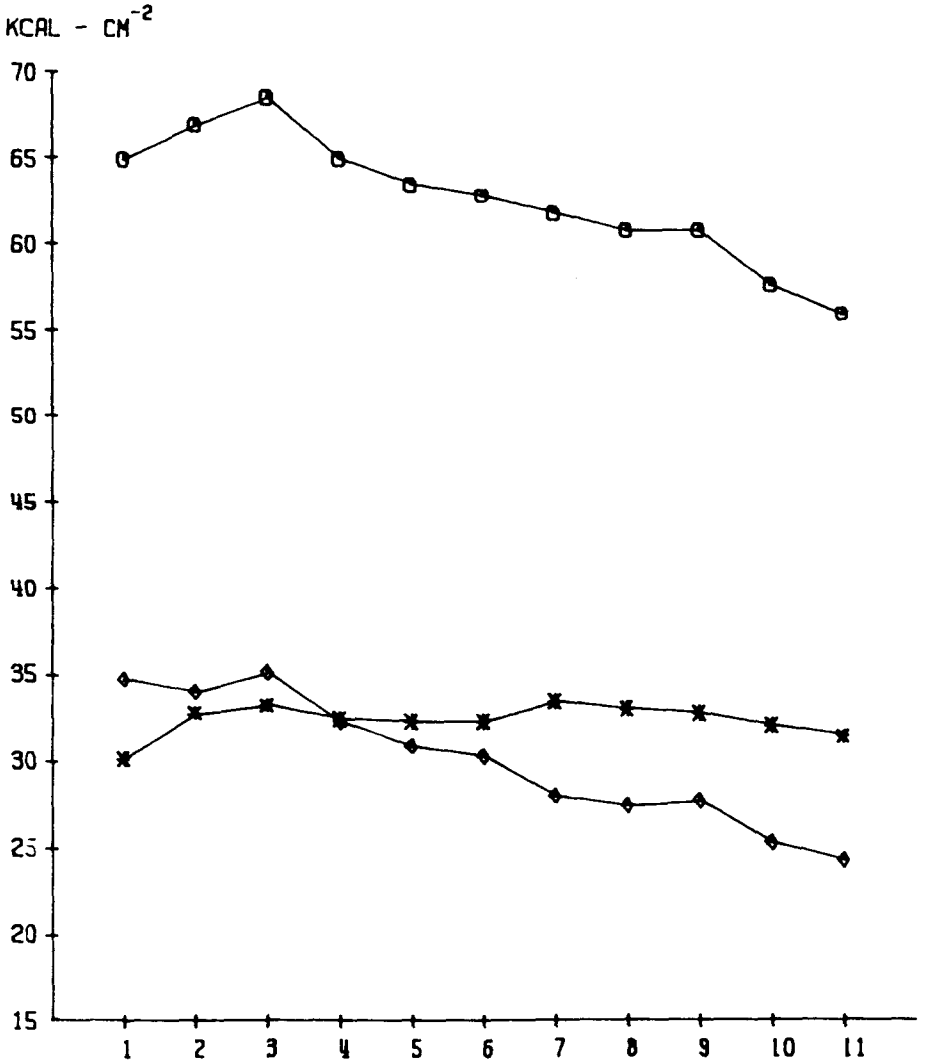

Figure 13. Cross-shelf distribution of Qs along Seward Line for December. Symbols represent same depth intervals as those in Figure 12.

variable in magnitude) throughout the year, surface water is continuously flowing shoreward. From October through March this water experiences a nearly continuous loss of heat. Close to shore katabatic conditions, as described by Reynolds (1978), will augment the heat loss. Because of convergence this cool surface water sinks at the coast. During summer the surface waters, warmed by solar radiation, converge on the coast and sink.

In light of these seasonal patterns of heat distribution and the deflection of the coastal jet by Kayak Island toward Middleton Island, it is doubtful that the alongshore thermal gradient computed from the MDO stations is representative of the average monthly gradient. Use of the MDO stations would tend to underestimate the gradient in winter and overestimate it in summer. In comparison with the gradients computed from SST data, the MDO gradients are substantially smaller in February and 4 to 6 times greater in May, July, August and September. These results qualitatively agree with the foregoing discussion except for March and May which one would expect to underestimate the gradient. Most likely the trajectory of the deflected coastal current is variable with respect to time and space. Although these results arouse suspicion concerning the representativeness of the MDO stations of the midshelf heat content, I am not implying that the gradients computed from the SST data are more accurate. A reliable assessment of the alongshore advection of heat awaits a more refined resolution of the kinematics of the shelf circulation.

The combined effects of surface heat exchange and coastal convergence result in annual temperature variations that are larger and penetrate to greater depths inshore than offshore. These influences are summarized in Figure 14. The circles represent the annual amplitude in Q_s (integrated over 100 m) for Station 1 through 11. The ranges decrease markedly from a high of 58 kcal cm^{-2} at the coast to about 25 kcal cm^{-2} within the Alaska Current. This decrease is nearly smooth except for the perceptively higher annual ranges for Stations 7 through 9. Royer (unpub. manuscript) shows evidence that the coastal current deflected by Kayak Island flows through the area. Furthermore, Niebauer *et al.* (1980) suggest that this is a region of frequent eddy activity. Both processes would enhance the annual variability in the thermal characteristics of this region of the shelf. Although the present data are not adequate to statistically resolve these perceived deviations, it seems probable that they are real. The asterisks represent the fraction of the annual range within this layer accounted for by the upper 50 m. The percentage attributable to the upper 50 m decreases sharply from 95% within the Alaska Current (Station 11) to 75% across the outer shelf (Stations 6 through 9). From Station 6 to the coast this percentage decreases monotonically. Because salinity is the primary determinant of density and precipitation and runoff exceed evaporation in all months, surface cooling is insufficient to promote deep convective overturn. Consequently, the cross-shelf variations portrayed in Figure 14 can be accounted for by the increasing magnitude of downwelling velocities from offshore to onshore.

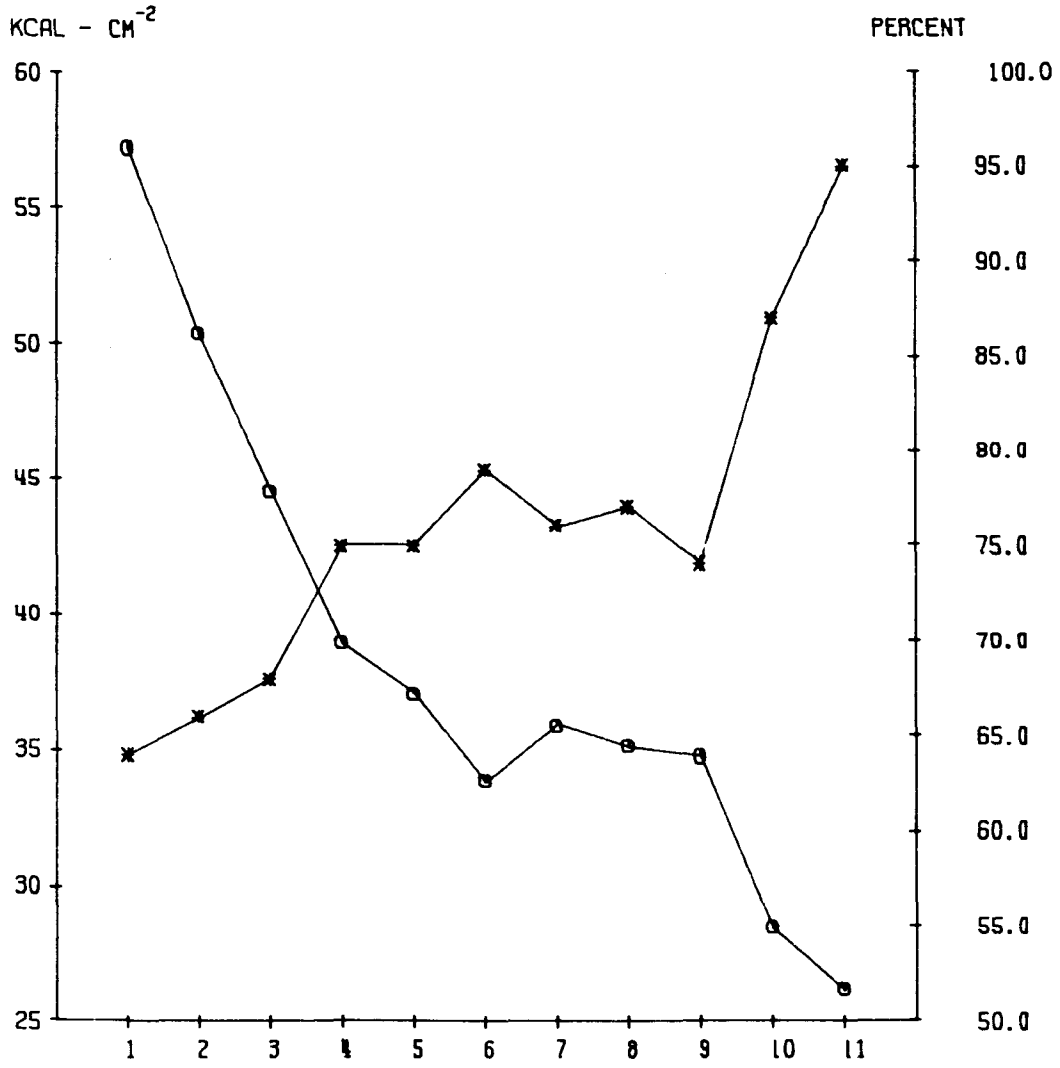

Figure 14. Annual range of Qs (0-100 m) along the Seward Line (circles). Fraction of annual amplitude of Qs accounted for in the 0-50 m interval expressed as percent (asterisks).

The spatial variation in downwelling velocities give rise to different propagation speeds of surface temperature anomalies to greater depths. This effect is illustrated by the phase differences ($\Delta\phi$) between temperatures at 10 and 100 m for the eleven stations along the Seward Line. By fitting the temperatures at the two depths to eq. (6) the phase angle, ϕ, is given by the arctangent of -B/A (Bloomfield, 1975). Figure 15 shows that the phase differences increase nearly linearly from a minimum of 8 degrees (days) at Station 1 to approximately 30 degrees (days) over the middle shelf to 45 degrees (1.5 months) near the Alaska Current. Thus mean monthly SST anomalies over the middle shelf would be reflected by thermal anomalies at 100 m approximately 1 month later, whereas the inshore region response is on the order of a week. Within the Alaska Current there is no detectable annual signal to temperature at 100 m, hence surface heating and cooling anomalies do not propagate to this depth.

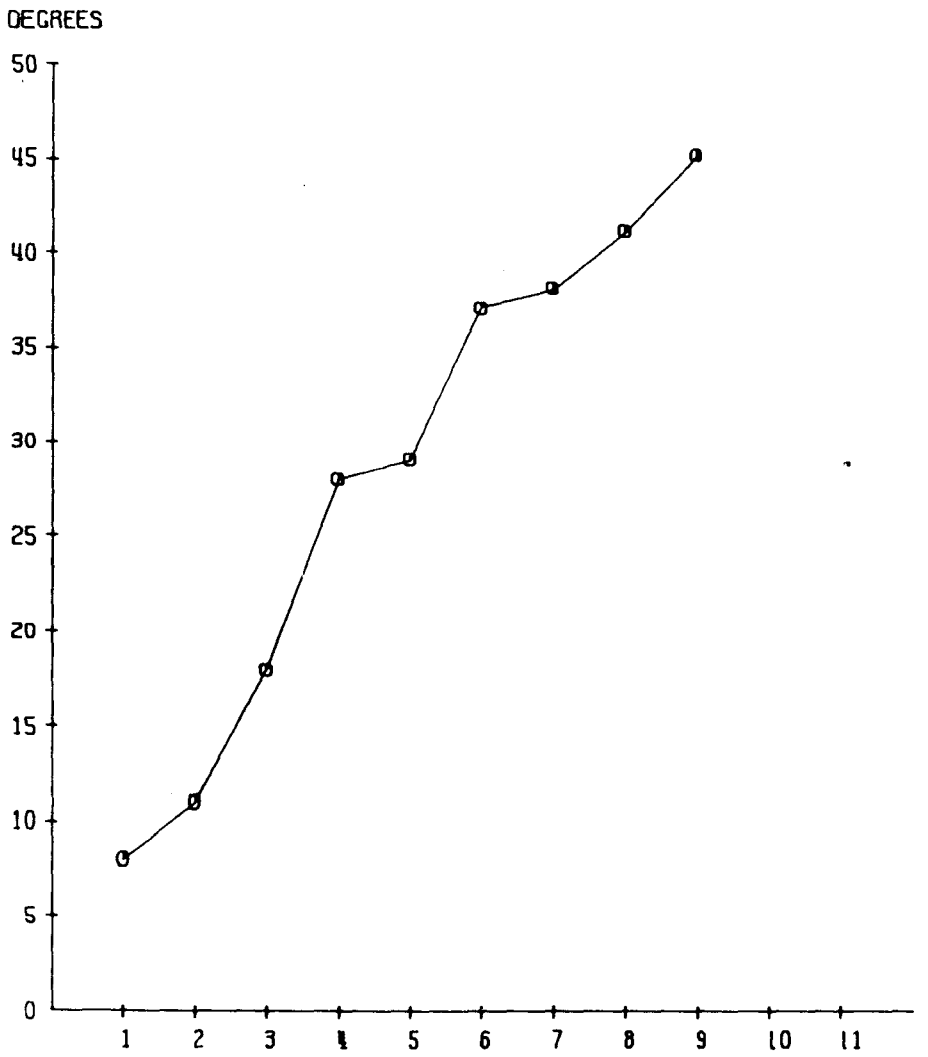

Figure 15. Phase difference, $\Delta\phi$, between temperature at 10 m and temperature at 100 m.

CHAPTER 6

SUMMARY AND CONCLUSIONS

Heat exchange on the shelf of the northwest Gulf of Alaska is, in all months, dominated by atmospheric heat fluxes. From April through September the ocean experiences a net gain of heat principally from radiation. From October through March the shelf water undergoes continuous cooling primarily via evaporative and conductive heat loss.

As a consequence of year-round downwelling velocities on the order of -1×10^{-4} cm sec^{-1}, vertical advection is the second most important route for the loss of heat from the upper 100 m.

In all seasons except late spring to mid-summer alongshore advection of heat represents a substantial fraction of the total heat gain for this region. This term is the most important heat source from October through January. During this period net radiation is near zero and the alongshore gradient and current velocities attain their annual maxima.

Cross-shelf advection and diffusion of heat are of minor importance throughout the year and generally counter each other. The inverse phase relationshp between these two terms is attributed to the influence of coastal convergence on the distribution of heat across the shelf. The year-round prevalence of onshore Ekman transport also explains the cross-shelf variation in the annual amplitude of heat content and the response times of deeper water to surface temperature anomalies. The annual ranges decrease and the deep water response time increases from inshore to offshore.

Attempts to correlate monthly sea surface temperature anomalies with anomalous monthly surface heat exchanged did not yield significant coefficients. This result must be regarded as tentative because of the small sample size used. However, because of the importance of the Alaska Current in the global distribution of heat and its proximity to the study area, thermal anomalies on the shelf may be more closely related to secular variation in mass transport or advection of thermal anomalies from elsewhere in the North Pacific. Other, more local, influences have also been suggested as contributing to thermal anomaly formation. These processes include the effect of eddies and meanders born from the Alaska Current and the effects of freshwater influx on the mixed layer depth.

REFERENCES

Arthur, R. S. 1965. On the calculation of vertical motion in Eastern Boundary currents from determination of horizontal motions. *J. Geophys. Res.* 70(12):2799-2803.

Bakun, A. 1975a. Coastal upwelling indices, west coast of North America, 1946-71. U.S. Dept. Comm. Natl. Oceanic Atmos. Admin. Tech. Rept. NMFS SSRF-671. 103 pp.

Bakun, A. 1975b. Daily and weekly upwelling indices, west coast of North America, 1867-73. U.S. Dept. Comm. Natl. Oceanic Atmos. Admin. Tech. Rept. NMFS SSRF-693. 114 pp.

Bathen, K. H. 1971. Heat storage and advection in the North Pacific Ocean. *J. Geophys. Res.* 76(3):676-686.

Bloomfield, P. 1975. *Fourier Analysis of Time Series: An Introduction.* John Wiley and Sons. New York. 258 pp.

Brower, W. A., H. F. Diaz, A. S. Prechtel, H. W. Searby and J. L. Wise. 1977. Climatic atlas of the outer continental shelf waters and coastal regions of Alaska, Vol. 1, Gulf of Alaska. U.S. Dept. Comm. Natl. Oceanic Atmos. Admin., Alaska Outer Continental Shelf Environmental Assessment Program, Final Rept. RU-317. 439 pp.

Bryden, H. L. 1978. Mean upwelling velocities on the Oregon continental shelf during summer 1973. *Est. Coastal Mar. Sci.* 7:311-327.

Businger, J. A. 1972. Turbulent transfer in the atmospheric surface layer. *In* D. A. Haugen (ed.), Workshop on Micrometeorology. American Meteorological Society, Boston, Mass. p. 67-100.

Clark, N. E. 1967. Report on an investigation of large-scale heat transfer processes and fluctuations of sea-surface temperature in the North Pacific Ocean. The Solar Energy Research Fund of the Massachusetts Institute of Technology, Cambridge, Mass. 268 pp.

Davis, R. E. 1976. Predictability of sea surface temperature and sea level pressure anomalies over the North Pacific Ocean. *J. Phys. Oceanog.* 6(3):249-266.

Deardorff, J. W. 1968. Dependence of air-sea transfer coefficients on bulk stability. *J. Geophys. Res.* 73(8):2549-2557.

Elliot, R. D. and T. B. Smith. 1949. A study of the effects of large blocking highs on the general circulation in the Northern Hemisphere westerlies. *J. Met.* 6(2):67-85.

Favre, A. and K. Hasselmann. 1978. Turbulent fluxes through the sea surface, wave dynamics, and prediction. NATO Conference on Turbulent fluxes through the sea surface, wave dynamics, and prediction. Paris, France, 1977. Plenum Press, New York. 677 pp.

Friehe, C. A. and C. H. Gibson. 1978. Estimates of the surface fluxes over the ocean. *In* A. Favre, K. Hasselmann (eds.), Turbulent fluxes through the sea surface wave dynamics, and prediction. NATO Conference. Paris, France, 1977. Plenum Press, New York. p. 67-77.

Hamilton, P. and M. Rattray, Jr. 1978. A numerical model of the depth-dependent, wind driven upwelling circulation on a continental shelf. *J. Phys. Oceanog.* 8(3):437-457.

Haney, R. L., W. S. Shiver and K. H. Hunt. 1978. A dynamical-numerical study of the formation and evolution of large scale ocean anomalies. *J. Phys. Oceanog.* 8(5):755-778.

Haugen, D. A. (ed.). 1973. Workshop on Micrometeorology. American Meteorological Society, Boston, Mass. 382 pp.

Hayes, S. P. 1979. Variability of current and bottom pressure across the continental shelf in the northeast Gulf of Alaska. *J. Phys. Oceanog.* 9(1):88-103.

Hayes, S. P. and J. D. Schumacher. 1976. Description of wind, current and bottom pressure variations on the continental shelf in the northeast Gulf of Alaska from February to May 1975. *J. Geophys. Res.* 81(36):6411-6419.

Huang, J. C. K. 1979. Numerical case studies for oceanic thermal anomalies with a dynamic model. *J. Geophys. Res.* 84(9):5717-5726.

Jacobs, W. C. 1951. The energy exchange between sea and atmosphere and some of its consequences. Bull. Scripps Institution of Oceanography, University of California, Vol. 6:27-122.

Klein, W. H. 1957. Principal tracks and mean frequencies of cyclones and anticyclones in the Northern Hemisphere. U.S. Weather Bureau, Res., Paper 40. 60 pp.

Klein, W. H. and J. S. Winston. 1958. Geographical frequency of troughs and ridges on mean 700 mb charts. *Mon. Wea. Rev.* 87(9):344-358.

Kraus, E. B. 1972. *Atmosphere-ocean interaction.* Oxford University Press, London. 275 pp.

Kraus, E. B. and J. S. Turner. 1967. A one-dimensional model of the seasonal thermocline. II The general theory and its consequences. *Tellus* 19:98-105.

Kondo, J. 1975. Air-sea bulk transfer coefficients in diabatic conditions. *Boundary-Layer Met.* 9:91-112.

Kondratyev, K. Ya. 1972. Radiation processes in the atmosphere. World Meteorological Organization, WMO-No. 309. 214 pp.

Livingstone, D. M. 1979. A statistical and spectral analysis of observed surface winds at three stations in the Gulf of Alaska. M.S. Thesis, University of Alaska, Fairbanks. 295 pp.

Livingstone, D. M. and T. C. Royer. 1980. An analysis of observed surface winds at Middleton Island, Gulf of Alaska. (Submitted to *J. Phys. Oceanog.*)

Manabe, S. and K. Bryan. 1969. Climate calculations with a combined ocean-atmosphere model. *J. Atmos. Sci.* 24:241-259.

Merlo, T. O. 1974. Thermal structure and calculated heat budget: Gulf of Alaska. M.S. Thesis, University of Alaska, Fairbanks. 31 pp.

Namias, J. 1963. Large scale air-sea interactions over the North Pacific from summer 1962 through the subsequent winter. *J. Geophys. Res.* 68(22):6171-6186.

Namias, J. 1968. The labile Gulf of Alaska cyclone--key to large scale weather modification elsewhere. Proceedings of the International Conference Cloud Physics, Toronto. pp. 735-743.

Namias, J. 1970. Macroscale variations in sea-surface temperatures in the North Pacific. *J. Geophys. Res.* 75(3):565-582.

Niebauer, H. J., J. Roberts and T. C. Royer. 1980. Currents near the shelf break in the northern Gulf of Alaska, 1976-77. (Submitted to *J. Geophys. Res.*)

O'Connor, J. F. 1964. Hemispheric distribution of 5-day mean 700-mb circulation centers. *Mon. Wea. Rev.* 92(6):303-315.

Okubo, A. and R. V. Ozmidov. 1970. Empirical dependence of the coefficient of horizontal turbulent diffusion in the ocean on the scale of the phenomenon in question. *Izv. Atmospheric and Oceanic Physics* 6(5):534-536.

Pond, S., G. T. Phelps, J. E. Paquin, G. McBean and R. W. Stewart. 1971. Measurements of the turbulent fluxes of momentum, moisture sensible heat over the ocean. *J. Atmos. Sci.* 28(6):901-917.

Reed, R. J. 1960. Principal frontal zones of the Northern Hemisphere in winter and summer. *Bull. Am. Met. Soc.* 41(11):591-598.

Reed, R. K. 1976. On estimation of net long-wave radiation from the oceans. *J. Geophys. Res.* 81(33):5793-5794.

Reed, R. K. 1977. On estimating insolation over the ocean. *J. Phys. Oceanog.* 7:482-485.

Reynolds, R. 1978. Near-shore meteorology. U.S. Dept. Comm. Natl. Oceanic Atmos. Admin. U.S. Dept. Int., U.S. Bur. Land Management Environmental Assessment of the Alaskan Continental Shelf: Annual Report Vol. 10 transport, RU 367:324-568.

Royer, T. C. 1975. Seasonal variations of waters in the northern Gulf of Alaska. *Deep-Sea Res.* 22:403-416.

Royer, T. C. 1979. On the effect of precipitation and runoff on coastal circulation in the Gulf of Alaska. *J. Phys. Oceanogr.* 9(3):555-563.

Royer, T. C. and R. D. Muench. 1977. On the ocean temperature distribution in the Gulf of Alaska, 1974-1975. *J. Phys. Oceanogr.* 7(1):92-99.

Royer, T. C., D. V. Hansen and D. J. Pashinski. 1979. Coastal flow in the northern Gulf of Alaska as observed by dynamic topography and satellite-tracked drogued drift buoys. *J. Phys. Oceanogr.* 9(4): 785-801.

Sadler, J. C., L. Oda and B. J. Kilonsky. 1976. Pacific Ocean cloudiness from satellite observations. Dept. Met. U. Hawaii. 137 pp.

Seckel, G. R. and F. H. Beaudry. 1973. The radiation from sun and sky over the North Pacific Ocean (abstract). *Trans. Am. Geophys. Union* 54:114.

Smith, P. C. 1978. Low frequency fluxes of momentum, heat, salt and nutrients at the edge of the Scotian shelf. *J. Geophys. Res.* 83: 4079-4096.

Thomson, R. E. 1972. On the Alaskan Stream. *J. Phys. Oceanogr.* 2:363-371.

U.S. Dept. Comm. Natl. Oceanic Atmos. Admin., Systems Development Office. 1976. Automatic surface data acquisition systems of the National Weather Service. Staff Document. 46 pp.

Weng, C. S. and R. L. Street. 1978. Transfer across an air-water interface at high wind speeds: the effect of spray. *J. Geophys. Res.* 83:2959-2969.

White, W. B. 1977. Secular variability in the baroclinic structure of the interior North Pacific from 1950-1970. *J. Mar. Res.* 35(3):587-607.

White, W. B. and T. P. Barnett. 1972. A servomechanism in the ocean/atmosphere system of the mid-latitude North Pacific. *J. Phys. Oceanogr.* 2(4):372-381.

White, W. B. and N. E. Clark. 1975. On the development of blocking ridge activity over the central North Pacific. *J. Atmos. Sci.* 32:489-502.

Winston, J. S. 1955. Physical aspects of rapid cyclogenesis in the Gulf of Alaska. *Tellus* 7(4):481-500.

Wooster, W. S. and J. L. Reid. 1963. Eastern Boundary Currents. *In* M. N. Hill (ed.), The Sea, Vol. 2. Interscience, New York. p. 253-280.

Wooster, W. A. and B. A. Taft. 1958. On the reliability of field measurements of temperature and salinity in the ocean. *J. Mar. Res.* 17:552-566.

Wyrtki, K. and K. Haberland. 1968. On the redistribution of heat in the North Pacific Ocean. *J. Oceanogr. Soc., Japan* 24(5):220-233.